

Geochemistry, Geophysics, Geosystems®

RESEARCH ARTICLE

10.1029/2021GC010308

Key Points:

- Nitrogen-isotope records of globally variable environmental change in the Frasnian–Famennian crisis
- Combination with age models highlights further variability in the onset of those changes
- Multi-proxy geochemistry highlights nutrient runoff as trigger of earliest anoxia

Supporting Information:

Supporting Information may be found in the online version of this article.

Correspondence to:

L. M. E. Percival,
lawrence.percival@vub.be

Citation:

Percival, L. M. E., Marynowski, L., Baudin, F., Goderis, S., De Vleeschouwer, D., Rakociński, M., et al. (2022). Combined nitrogen-isotope and cyclostratigraphy evidence for temporal and spatial variability in Frasnian–Famennian environmental change. *Geochemistry, Geophysics, Geosystems*, 23, e2021GC010308. <https://doi.org/10.1029/2021GC010308>

Received 16 DEC 2021
Accepted 8 FEB 2022

Combined Nitrogen-Isotope and Cyclostratigraphy Evidence for Temporal and Spatial Variability in Frasnian–Famennian Environmental Change

L. M. E. Percival¹ , L. Marynowski² , F. Baudin³ , S. Goderis¹ , D. De Vleeschouwer⁴ , M. Rakociński² , K. Narkiewicz⁵ , C. Corradini⁶ , A.-C. Da Silva⁷ , and P. Claeys¹ 

¹Analytical, Environmental, and Geochemistry (AMGC), Vrije Universiteit Brussel, Brussels, Belgium, ²Institute of Earth Sciences, University of Silesia in Katowice, Sosnowiec, Poland, ³Institut des Sciences de la Terre de Paris (ISTeP), Sorbonne Université, Paris, France, ⁴Institute of Geology and Paleontology, University of Münster, Münster, Germany, ⁵Polish Geological Institute–National Research Institute, Warsaw, Poland, ⁶Dipartimento di Matematica e Geoscienze, Università di Trieste, Trieste, Italy, ⁷Sedimentary Petrology Laboratory, Liège University, Liège, Belgium

Abstract Widespread marine anoxia triggered by the runoff and recycling of nutrients was a key phenomenon associated with the Frasnian–Famennian (FF) mass extinction. However, the relative importance of global-scale processes versus local influences on site-specific environmental change remains poorly understood. Here, nitrogen-isotope ($\delta^{15}\text{N}$) trends are combined with organic-biomarker, phosphorus, and Rock-Eval data in FF sites from the USA (H-32 core, Iowa), Poland (Kowala Quarry), and Belgium (Sinsin). Up-to-date cyclostratigraphic age models for all three sites allow the nature and timing of changes to be precisely compared across the globe. Negative $\delta^{15}\text{N}$ excursions across the FF interval from the H-32 core and Kowala correlate with geochemical evidence for euxinic, phosphorus-rich, water columns, and possible cyanobacterial activity, suggestive of increased diazotrophic N fixation, potentially coupled with ammonium assimilation at the latter site. By contrast, previously studied sites from Western Canada and South China document enhanced water-column denitrification around the onset of the Upper Kellwasser (UKW) Event, re-emphasizing the geographical heterogeneity in environmental perturbations at that time. Moreover, environmental degradation began >100 kyr earlier in Poland, coeval with a major increase in bioavailable phosphorus supply, than in Iowa, where no such influx is recorded. These regional differences in both the timing and nature of marine perturbations during the FF interval likely resulted from the variable influx of terrigenous nutrients to different marine basins at that time, highlighting the importance of local processes such as terrestrial runoff in driving environmental degradation during times of climate cooling such as the UKW Event.

Plain Language Summary The Frasnian–Famennian mass extinction, ~372 million years ago, marked one of the most severe biological crises in Earth's history. The extinction has been linked to rapid climate changes and reduced seawater oxygen levels across the global ocean. However, the degree to which environmental stress was globally versus locally controlled remains unclear. This study presents geochemical markers of water-column oxygenation and nutrient cycling (nitrogen isotopes, phosphorus contents, organic biomarkers) at three localities, the H-32 core (Iowa, USA), the Kowala Quarry (Poland), and Sinsin (Belgium). The unique feature of these records is the existence of precise age-depth models, allowing direct comparison of the timing of environmental changes between these sites, and with other key sections from Western Canada and South China. It is shown that whilst the H-32 core and Kowala indicate possible increases in cyanobacterial nitrogen fixation under phosphorus-rich, oxygen- and nitrate-depleted conditions, other sites show markedly different nitrogen-cycle disturbances, such as enhanced water-column denitrification. Additionally, environmental stress commenced earlier in Kowala than elsewhere, coincident with elevated phosphorus influx to that setting. These regional variations in the timing and nature of environmental perturbations emphasize the importance of local processes such as terrestrial nutrient runoff in causing the Frasnian–Famennian extinction.

1. Introduction

The Upper Kellwasser (UKW) Event featured one of the “Big Five” Phanerozoic mass extinctions, during the Frasnian–Famennian (FF) transition (~372 Ma), alongside worldwide environmental disturbances (see Carmichael et al., 2019). The event began ~150 kyr prior to the end of the Frasnian Stage (De Vleeschouwer et al., 2017),

© 2022. The Authors.

This is an open access article under the terms of the [Creative Commons Attribution License](https://creativecommons.org/licenses/by/4.0/), which permits use, distribution and reproduction in any medium, provided the original work is properly cited.

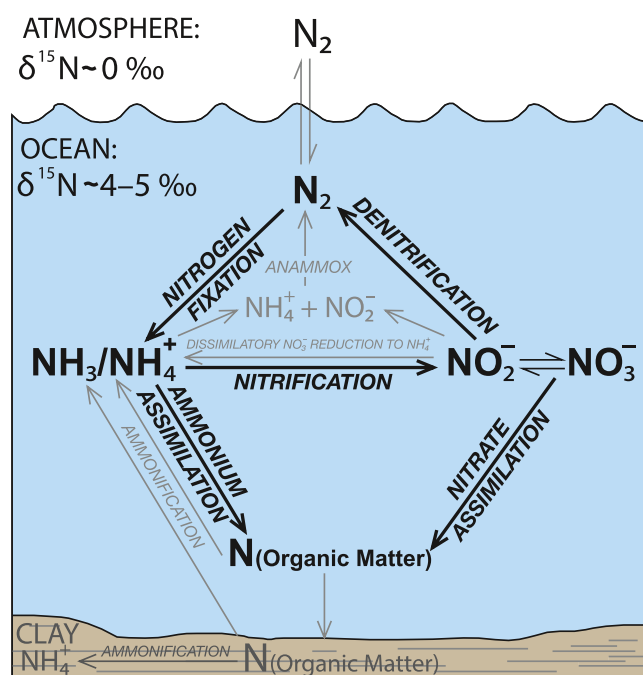


Figure 1. Simplified schematic of the modern nitrogen cycle, adapted from Sun et al. (2019). The modern-day average isotopic compositions of the ocean (4–5‰) and atmosphere (0‰) are indicated (Altabet, 2007). Arrows indicate (bio)chemical processes that result in the transformation of nitrogen species. The key processes discussed in this work that are likely to have changed, and potentially impacted seawater $\delta^{15}\text{N}$ values, during the UKW Event are indicated in bold. See overview by Sigman and Fripiat (2019) for a more detailed diagram of the marine nitrogen cycle and associated isotopic fractionations.

and is marked in the global stratigraphic record by a positive excursion of up to 4‰ in the carbon-isotope composition of both bulk organic ($\delta^{13}\text{C}_{\text{org}}$) and carbonate ($\delta^{13}\text{C}_{\text{carb}}$) material (e.g., Joachimski et al., 2002). Thus, the Upper Kellwasser (UKW) Event is generally regarded as having been characterized by widespread marine anoxia–euxinia and an associated increase in organic-matter burial (e.g., Bond et al., 2004; Carmichael et al., 2019; Pujol et al., 2006). The crisis was also marked by a spell of pronounced climate cooling (e.g., Balter et al., 2008; Joachimski & Buggisch, 2002). Whilst the ultimate trigger of the event remains debated (see recent reviews by Bond & Grasby (2017), Carmichael et al. (2019), Qie et al. (2019), and Racki (2020)), the increased runoff of terrigenous nutrients such as phosphorus (P) from intense continental weathering has long been proposed as the key driver of the recorded marine environmental degradation, potentially related to one or both of orogenic belt formation and the expansion of vascular-rooted land plants (e.g., Algeo et al., 1995; Averbuch et al., 2005). However, the nature and severity of the environmental perturbations apparently varied worldwide (Bond et al., 2004; Carmichael et al., 2019; Pujol et al., 2006; Whalen et al., 2015). Thus, the extent to which environmental changes were global or local in scale, and synchronous in their onset and duration, remains unclear.

This study integrates cyclostratigraphic timescales of three Frasnian–Famennian (FF) archives with bulk nitrogen content and isotopic composition ($\delta^{15}\text{N}$) data to investigate geographic variability in the timing/severity of environmental perturbations during the Upper Kellwasser (UKW) Event. Diazotrophic fixation of atmospheric nitrogen is the main source of the element to the ocean, which is rendered isotopically light (–1–0‰) by a minor isotopic fractionation attendant with this process. Runoff of terrestrial organic matter and/or clay material acts as an additional source in settings proximal to the shoreline. Autotrophic nitrate assimilation and (in oxygen-depleted settings) denitrification/anammox are the main sinks of nitrate/nitrite and ammonia/ammonium, with water-column denitrification in particular strongly fractionating in favor of ^{14}N , increasing the $\delta^{15}\text{N}$ value of the resid-

ual nitrogen pool (Figure 1; see also Sigman & Fripiat, 2019, and references therein). The balance between these processes is reflected by a modern-day average oceanic $\delta^{15}\text{N}$ value of ~4–5‰ for dissolved inorganic nitrogen (Altabet, 2007). However, some marine environments feature somewhat lower $\delta^{15}\text{N}$ values. In the North Atlantic Ocean, a high abundance of key nutrients such as phosphorus and iron, combined with low nitrate concentrations, promote conditions ecologically favorable for diazotrophs, such as cyanobacteria, resulting in a higher input of isotopically light fixed nitrogen (Marconi et al., 2017). Additionally, in highly reducing settings such as the Cariaco Basin, near-total consumption of available nitrate results in both enhanced N fixation and limited water-column denitrification (Thunell et al., 2004). In the geological past, the average oceanic $\delta^{15}\text{N}$ value apparently deviated significantly from that of the modern-day, particularly in greenhouse worlds, with sedimentary records of those times typically recording nitrogen-isotope ratios below ~4–5‰ (e.g., Algeo et al., 2014; Jenkyns, 2010; Kast et al., 2019; Tuite et al., 2019).

The hypothesized lower limit of seawater $\delta^{15}\text{N}$ due to N fixation is –1‰ for modern settings (see Higgins et al., 2012; Zhang et al., 2014; and references therein). However, some bulk sedimentary records document $\delta^{15}\text{N}$ values of –3‰ or lower, from both geologically recent settings (e.g., Mediterranean Sapropels; Elling et al., 2021) and more ancient ones (e.g., Paleocene–Eocene shallow-water Peri-Tethys seaway; Junium et al., 2018; open-ocean archives of Cenomanian–Turonian oceanic anoxic event—OAE 2; Jenkyns et al., 2007; Junium & Arthur, 2007; Ruvalcaba Baroni et al., 2015). These atypically low $\delta^{15}\text{N}$ values are generally attributed to a cessation of nitrification in a severely oxygen-depleted (likely euxinic) water column, enabling the build-up and assimilation of ammonium by phytoplankton to become a significant pathway in local nitrogen cycling (Higgins et al., 2012). Alternatively, it has been proposed that nitrogen fixation can result in $\delta^{15}\text{N}$ values below –1‰ if one or both of iron- (Fe-) and vanadium- (V-) based nitrogenases are utilized in place of the typical

Frasnian–Famennian (372 Ma)

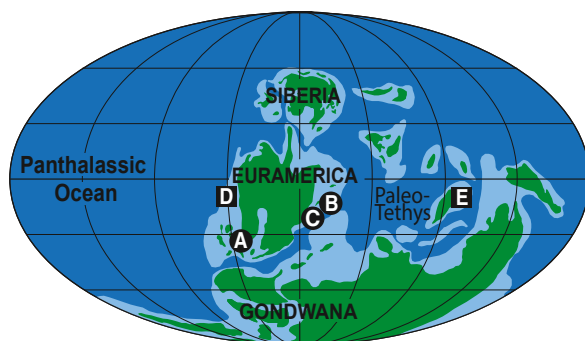


Figure 2. Late Devonian paleogeographic map, adapted from Percival et al. (2019). Sites studied for both cyclostratigraphy (De Vleeschouwer et al., 2017) and $\delta^{15}\text{N}$ trends (circles: this study; squares: Whalen et al., 2015), are marked as follows: (A) H-32 core, Iowa, USA; (B) Kowala Quarry, Poland; (C) Sinsin, Belgium; (D) Section C, Alberta, Canada; (E) Fuhe, Guangxi Province, S. China.

molybdenum- (Mo-) nitrogenase (Zhang et al., 2014), although the importance of these alternative enzymes in marine settings remains unclear.

Here, three new records of sedimentary $\delta^{15}\text{N}$ trends across the Frasnian–Famennian (FF) transition are presented (Figure 2), from the H-32 core (Illinois Basin, Iowa, USA), Kowala Quarry (Chęciny-Zbrza Basin, Poland), and Sinsin (Namur-Dinant Basin, Belgium), with the H-32 and Kowala datasets complemented by analyses of Rock-Eval parameters, organic-biomarkers, and phosphorus and aluminum contents. Both the FF boundary and UKW Level are documented at each location by conodont biostratigraphy and $\delta^{13}\text{C}$ trends (De Vleeschouwer et al., 2017; Joachimski et al., 2001; Percival et al., 2019; Sandberg et al., 1988; *this study*). Crucially, all three locales feature cyclostratigraphic age models, enabling temporal correlation of geochemical trends between them and two other sites previously studied for $\delta^{15}\text{N}$ and cyclostratigraphy (Section C, Western Canada Sedimentary Basin, Alberta, Canada, and Fuhe, Yangshuo Basin, Guangxi Province, S. China; Figure 2). Thus, a comparative timescale for the onset and nature of nitrogen-cycle perturbations associated with the UKW Event can be constructed for these records, and a detailed history of how environmental degradation proceeded in different regions established.

2. Study Areas

2.1. H-32 Core (Illinois Basin, Iowa, USA, 40°28'19" N, 91°28'8" W)

The Iowa and Illinois basins were effectively a single epicontinental basin in the Late Devonian (referred to here as the Illinois Basin), one of many such environments that existed across Euramerica during that time. The H-32 core drilled sediments deposited on the western slope of this basin, predominantly consisting of carbonate-poor siltstones and shales (Witzke & Bunker, 2002). The FF boundary is defined by conodont biostratigraphy (Day & Witzke, 2017; De Vleeschouwer et al., 2017), and is placed just stratigraphically above a transition from the relatively organic-lean (typically <0.5 wt% total organic carbon; TOC) green and gray siltstones and marls of the Sweetland Creek Shale to much more organic-rich (2–5 wt% TOC) mudstones of the Grassy Creek Shale (Day & Witzke, 2017; Liu et al., 2021; Witzke & Bunker, 2002). However, there is no biostratigraphic evidence (i.e., missing conodont zones) of a major disconformity associated with this abrupt lithological change, and a gradual increase in $\delta^{13}\text{C}_{\text{org}}$ (assumed to mark the UKW Level) across this transition shows no sharp step in values that would suggest missing strata. Thus, the H-32 core record of the FF interval is thought to be relatively complete. The lowermost Famennian strata of the Grassy Creek Shale are interbedded with preserved ash layers, indicative of local volcanic activity in the immediate aftermath (at least) of the FF extinction (Day & Witzke, 2017). The preservation of organic-rich shales around the FF boundary suggests the development/expansion of oxygen-depleted conditions in the Illinois Basin during the transition, consistent with previous geochemical models suggesting that this marine basin (and several others across Euramerica) were hydrographically restricted at that time (Algeo et al., 2007; Algeo & Tribouillard, 2009), hindering seawater replenishment and promoting stratification and deoxygenation.

A cyclostratigraphic timescale has been developed for the FF interval of the H-32 core, based on magnetic susceptibility and carbon-isotope data, together with conodont biostratigraphy (Da Silva et al., 2020; De Vleeschouwer et al., 2017). The new $\delta^{13}\text{C}_{\text{org}}$ data set for the H-32 core reported by Liu et al. (2021), whilst of lower resolution than the record of De Vleeschouwer et al. (2017), spans a broader stratigraphic range and suggests that the base of the isotopic excursion associated with the UKW Event is stratigraphically lower than previously assumed. As a key chemostratigraphic anchor point in defining the Frasnian–Famennian timescale around the world, this repositioned base of the $\delta^{13}\text{C}$ excursion allows for the cyclostratigraphic age model of the H-32 core, and its correlation with the other FF records in De Vleeschouwer et al. (2017) and Da Silva et al. (2020), to be refined more accurately. This chemostratigraphic adjustment is detailed in Table S1 in Supporting Information S1: the carbon-isotope-based tie-point immediately below the UKW excursion was originally placed at 8.19 m in Da Silva et al. (2020) and De Vleeschouwer et al. (2017), but because the base of the $\delta^{13}\text{C}_{\text{org}}$ shift has been revised stratigraphically down-core, the anchor point has likewise been placed 55 cm deeper than in the

previous two studies (at 7.64 m). Consequently, for the upper part of the H-32 core, the five age-depth tie-points retained by Da Silva et al. (2020) from the original De Vleeschouwer et al. (2017) model are revised to fit the global cyclostratigraphic framework while remaining consistent with the site-to-site chemostratigraphic correlations following the redefining of the base of the UKW $\delta^{13}\text{C}$ excursion in the H-32 core. In the lower part of the record, between 1.8 and 5.0 m, the age-depth relationships remain unaffected. This revised timescale provides relative ages with respect to the FF boundary, that are up to 140 kyr younger for some strata than the estimates of Da Silva et al. (2020) and De Vleeschouwer et al. (2017), with the maximum difference at the adjusted correlation point just below the UKW Level.

2.2. Kowala Quarry (Chęciny–Zbrza Basin, Poland, 50°47'42" N, 20°33'43" E)

The Chęciny–Zbrza intra-shelf basin was part of an extensive carbonate platform that covered more than 500 km across the northeastern part of Euramerica. While the basin was likely hydrographically restricted to some degree during the FF transition (Percival et al., 2019), a sufficient connection to the global ocean remained for marine organisms to migrate to and from the region, enabling the application of global conodont biostratigraphy (Szulczewski, 1996). The best studied sedimentary archive of the Chęciny–Zbrza Basin comes from the Kowala Quarry (hereafter termed Kowala), an actively worked site near Kielce in Poland, which exposes a relatively expanded Frasnian (upper Devonian) through to basal Tournaisian (lowest Carboniferous) stratigraphic sequence (Szulczewski, 1996). This study utilizes the sample-set investigated by Percival et al. (2019, 2020), which features a better-preserved FF boundary layer than most other Kowala records. The FF horizon has been identified on the basis of a thin chertiferous layer that marks the level throughout the quarry (Bond et al., 2004; Racki et al., 2002), together with new conodont biostratigraphy for this study (Table S2 in Supporting Information S1), following the zonations of Girard et al. (2005), Klapper and Kirchgasser (2016), and Spalletta et al. (2017). Just stratigraphically below the boundary, a switch from limestones to increasingly organic-rich shales, correlative with the globally documented carbon-isotope excursion, broadly indicates the UKW Level (Percival et al., 2019; *this study*), as also reported for another Kowala section (Joachimski et al., 2001). Increased nutrient (especially phosphorus) input and primary productivity in the Chęciny–Zbrza Basin during the FF transition, and the development of anoxic–euxinic conditions, have been reported by numerous works (e.g., Bond et al., 2004; Bond & Zatoń, 2003; Joachimski et al., 2001; Marynowski et al., 2011; Percival et al., 2020; Pujol et al., 2006; Racki et al., 2002).

A cyclostratigraphic age model exists for Kowala (De Vleeschouwer et al., 2013), although it was determined from another sample set, rather than the new record used in this study. However, both of the records feature a well-defined FF boundary (based on conodont biostratigraphy), and a clear positive carbon-isotope excursion in uppermost Frasnian strata, including a sharp turning point from gradually rising $\delta^{13}\text{C}_{\text{org}}$ values to a much sharper increase (Figure S2 in Supporting Information S1), which could potentially be interpreted as marking the onset of globally enhanced organic-carbon burial (e.g., Joachimski et al., 2002). Regardless, if the sharp increase in $\delta^{13}\text{C}_{\text{org}}$ values is interpreted to be stratigraphically equivalent in both sample sets, then the top 2.35 m of Frasnian strata between these two horizons in the old Kowala section can be stratigraphically correlated with the uppermost 90 cm of Frasnian sediments in the new record (see Text S1 and Figure S2 in Supporting Information S1). These strata are thought to represent ~100 kyr of time (De Vleeschouwer et al., 2013). Consequently, an average sedimentation rate of 0.90 cm/kyr is calculated for the top 90 cm of the Frasnian in the new record, and subsequently assumed for the rest of the studied interval (i.e., broadly constant sedimentation rate).

2.3. Sinsin (Namur-Dinant Basin, Belgium, 50°16'33" N, 5°14'8" E)

The FF stratigraphic interval recorded at Sinsin forms part of the southern rim of the Dinant Synclinorium, in the Namur-Dinant Basin (Casier & Devleeschouwer, 1995). The section consists primarily of marlstones and mudstones interbedded sporadically with limestones, with conodont biostratigraphy defining the FF boundary to within a 10–15 cm stratigraphic interval between the highest appearance of *A. ubiquitus* and lowest occurrence of *P. triangularis* (Casier & Devleeschouwer, 1995; Sandberg et al., 1988). A positive excursion in $\delta^{13}\text{C}_{\text{carb}}$ stratigraphically below the FF boundary marks the onset of the UKW Event (De Vleeschouwer et al., 2017), and high-resolution $\delta^{13}\text{C}_{\text{carb}}$ and magnetic-susceptibility data from Sinsin, integrated with similar datasets from other Late Devonian archives, have been used to construct a cyclostratigraphic timescale for the site (Da Silva et al., 2020; De Vleeschouwer et al., 2017). A shift towards locally deoxygenated (at least hypoxic) conditions during the FF transition has been proposed on the basis of a lithological change to dark gray mudstones (Casier

& Devleeschouwer, 1995), ostracod fossils indicative of such an environment (Casier, 2017), and the reported presence of biomarkers consistent with anoxic or even euxinic bottom waters (Kaiho et al., 2013), although TOC contents are extremely low throughout the Sinsin strata (typically <0.1 wt%, and never above 0.2 wt%; Kaiho et al., 2013; *this study*). Anoxic marine conditions have also been reported for other nearby Belgian sites (e.g., Claeys et al., 1996).

3. Materials and Methods

Decarbonated sedimentary samples were analyzed on a Nu Instruments Horizon 2 isotope-ratio mass spectrometer (IRMS) coupled to a Eurovector elemental analyzer EuroEA3000 at the Vrije Universiteit Brussel (VUB; Belgium) to determine the contents of total nitrogen (TN), TOC, and their isotopic compositions ($\delta^{15}\text{N}$, and $\delta^{13}\text{C}_{\text{org}}$). Approximately 1–2 g of homogenized sample powder were decarbonated in 10 ml of 10% HCl at room temperature for 3 hr (with each sample acid-treated twice and subsequently rinsed three times with milli-Q water before drying at 50°C), with the precise mass taken before and after acidification to calculate the percentage removed. Carbon and nitrogen concentrations of the decarbonated samples were determined together; these results were converted to TOC and TN contents of the bulk samples by accounting for the difference in sample mass before and after decarbonation. Based on these results, the values of $\delta^{15}\text{N}$ and $\delta^{13}\text{C}_{\text{org}}$ were determined, separately, for the decarbonated samples, using sufficient mass of powder to obtain a 4–5 nA peak ($^{44}\text{CO}_2$ and $^{28}\text{N}_2$ masses). Data calibration and determination of the accuracy and reproducibility/repeatability of measurements was carried out using the international reference materials IAEA-CH-6 (sucrose), IAEA-N1 (ammonium sulfate), and multiple certified reference materials calibrated against international standards: IA-R041 (L-alanine), IVA33802151 (organic-rich sediment), IVA33802153 (organic-poor soil). Repeated analysis of the standards across all instrument runs indicated analytical uncertainty typically better than ± 0.1 wt% (1 SD) for carbon and nitrogen contents, and $\pm 0.2\text{‰}$ (1 SD) for isotopic compositions. A subset of 25 untreated bulk powders from across the three study sites were also analyzed, to test whether the acid treatment resulted in a significant change in the measured $\delta^{15}\text{N}$ value of sedimentary rock samples.

For subsets of H-32 rocks, Rock-Eval data were generated at the Institute of Earth Sciences of Sorbonne University, Paris (France), and phosphorus (P_{tot}) and aluminum (Al) contents determined on a Thermo Scientific Element 2 sector field inductively coupled plasma mass spectrometer (ICP-MS) at the Vrije Universiteit Brussel (VUB). 50–70 mg of bulk homogenous powder were analyzed for Rock-Eval parameters following the protocols of Behar et al. (2001), depending on the TOC content of the sample. The Rock-Eval analyses determined both organic and inorganic carbon contents, together with the hydrogen index (HI), oxygen index (OI) and temperature of maximum hydrocarbon generation (T_{max}), which are jointly used to characterize the kerogen type and maturation level of organic matter (Espitalié et al., 1985). For major element analyses, 100 mg of powdered sample were digested using inverse aqua regia (3:1 mixture of concentrated subboiled HNO_3 :HCl by volume), with further digestion steps using concentrated subboiled hydrofluoric and nitric acids. Aluminum (Al) and P_{tot} were measured in medium-resolution mode of the instrument, externally calibrated against mixed-element solution standards. Two reference materials, BE-N and NISTSRM1646, were analyzed in the same batch to monitor sample-matrix influence, and, together with duplicated digestions, indicated accuracy and overall data reproducibility within 10% relative standard deviation (1 SD).

Organic compounds were extracted with a Dionex Accelerated Solvent Extractor 350, using a 1:1 (by volume) dichloromethane (DCM)/methanol mixture, and separated into aliphatic, aromatic, and polar fractions by modified column chromatography. Three eluents were used for fraction collection: *n*-pentane, *n*-pentane and dichloromethane (DCM) (7:3 by volume), and dichloromethane (DCM) and methanol (1:1 by volume) for the aliphatic, aromatic, and polar fractions, respectively. A blank sample (baked sand) was prepared for analysis using the same procedure. The extracted compounds were analyzed by an Agilent Technologies 7890A gas chromatograph coupled to an Agilent 5975C Network gas chromatography mass spectrometer (GC-MS) at the University of Silesia, and gas chromatography-tandem mass spectrometry (GC-MS/MS) system from Bruker, SCION triple quadrupole (SCION-TQ) series, at the Łukasiewicz Research Network, Wrocław (both Poland). For GC-MS analyses, the mass spectrometer was operated in the electron impact mode (ionization energy 70 eV), and spectra recorded from m/z 45–550 (0–40 min) and m/z 50–700 (>40 min). Aryl and diaryl isoprenoids were separated on a nonpolar HP5-MS silica column (60 m \times 0.32 mm inner diameter, 0.25 μm film thickness) coated with a chemically bonded phase of 5% phenyl and 95% methylsiloxane. Helium was used as a gas carrier, with a constant

flow mode (2.6 mL/min). The GC oven temperature was programmed from 45°C (1 min) to 100°C at 20°C/min, then to 300°C (held for 60 min) at 3°C/min. Hopanes and methylhopanes were separated on a semi-polar DB17-MS silica column (60 m × 0.25 mm inner diameter, 0.25 µm film thickness) coated with a chemically bonded phase of 50% phenyl and 50% methylsiloxane (after Marynowski et al., 2011). For biomarker analyses carried out on the GC-MS/MS system, samples were introduced into a gas chromatograph equipped with J&W HP5-MS (60 m × 0.32 mm inner diameter, 0.25 µm film thickness), coated with a chemically bonded phase of 5% phenyl, 95% methylsiloxane. The oven temperature was set at 40°C for 1 min, before being increased to 200°C at 20°C/min, and then 280°C at 1°C/min, with an isothermal hold for 2 min. The total run time was 91 min. 1 µL of sample was implemented by the injection port, with the temperature maintained at 250°C. The MS ion source temperature was set as constant at 250°C. Argon was used as a collision gas. Analysis of the blank baked-sand sample yielded only trace amounts of phthalates, likely derived from the concentrated solvents. Organic compounds including isorenieratane and methylhopanes were identified based on literature data (Clifford et al., 1998; Grice et al., 1997; Koopmans et al., 1996; Summons et al., 1999; Summons & Jahnke, 1990; Summons & Powell, 1987). To calculate the concentration of isorenieratane within the organic carbon of a sample, TOC contents were determined using the difference between total carbon (combusted under oxygen) and total inorganic carbon (reacted with 15% HCl) measured by infrared cell detection on an Eltra CS-500 IR analyzer, calibrated against Eltra standards. An internal standard (phenylindene) was added to the extracts before separation. Analytical uncertainty was better than ±2% for total carbon and ±3% for total inorganic carbon.

4. Results

Sedimentary TN contents increase from <0.1 wt% in background strata to up to 0.17 wt% and 0.23 wt% across FF boundary strata of the H-32 and Kowala records, respectively (Figures 3a and 3b). For both archives, this rise in TN broadly matches a previously reported increase in TOC contents (Liu et al., 2021; Percival et al., 2019, 2020). In contrast, both TOC and TN contents are extremely low (<0.1 wt%) throughout the studied interval at Sinsin (Figure 3c). HI and OI values for organic-rich samples from the H-32 core are generally between 500 and 600 mgHC/gTOC and <25 mgCO₂/gTOC, respectively, with an average T_{\max} of 432°C, consistent with immature Type II kerogen (Figure 4), and the Rock-Eval determined TOC data match the previously published isotope-ratio mass spectrometer (IRMS) values very well ($R^2 > 0.99$; $p < 0.001$).

Background Frasnian $\delta^{15}\text{N}$ values at all three sites are below those of modern-day seawater: ~2–3‰ for the H-32 core and Sinsin, and <0‰ at Kowala (Figure 3). Uppermost Frasnian strata of the H-32 and Kowala records document negative excursions in $\delta^{15}\text{N}$ values, from averages of 2.3‰ and −0.7‰ to mean values of 0.7‰ and −2.0‰, respectively (Figures 3a and 3b), with these lower values continuing into the lowermost Famennian. By contrast, $\delta^{15}\text{N}$ values remain relatively consistent (mean 2.4‰) throughout the studied interval from Sinsin (Figure 3c). $\delta^{15}\text{N}$ values of the subset of non-acidified samples showed a clear linear correlation with those of acidified aliquots of the same powder ($R^2 = 0.97$; $p < 0.001$; mean net offset = 0.04‰), (Figure S4 in Supporting Information S1). Thus, the acid treatment of the samples has not significantly affected their nitrogen-isotope composition or produced the documented stratigraphic trends. $\delta^{13}\text{C}_{\text{org}}$ values for Sinsin samples range from −28.11‰ to −23.20‰, but like $\delta^{15}\text{N}$, show no stratigraphic trend, with the characteristic FF boundary $\delta^{13}\text{C}$ positive excursion not clearly documented (Figure S5 in Supporting Information S1). New $\delta^{13}\text{C}_{\text{org}}$ data from Kowala are comparable to the data set presented in Percival et al. (2019).

Phosphorus contents for H-32 samples range from 89 to 904 µg/g, with P_{tot}/Al ratios between 1.3×10^{-3} and 1.4×10^{-2} (Figure 3a). The highest P_{tot} and P_{tot}/Al (g/g) values are recorded slightly below the FF boundary, but are generally lower than those previously determined for Kowala (Percival et al., 2020), and the P_{tot}/Al ratios are below the Post-Archean shale average (~0.01; Taylor & McLennan, 1995), apart from one sample, which only just exceeds it. However, trends in TOC/ P_{tot} molar ratios for the H-32 core are more comparable with those of Kowala, rising to approximately 500 in uppermost Frasnian–lowermost Famennian strata (Figures 3a and 3b).

An increase in both isorenieratane (from an average of 1.2 µg/g TOC to a maximum of 92.8 µg/g TOC) and 2-methyl-hopane (from mean 7.2% to maximum 17.3%) concentrations is detected just below the FF boundary at Kowala, broadly correlative with the rise in TOC content and negative excursion in $\delta^{15}\text{N}$ at that site (Figure 3b). Both biomarkers are also detected in the organic-rich Grassy Creek Shale strata of the H-32 core (8.7–76.1 µg/g TOC of isorenieratane; 1.5%–5.9% of 2-methyl-hopane; Figure 3a). It is assumed that the Grassy Creek strata

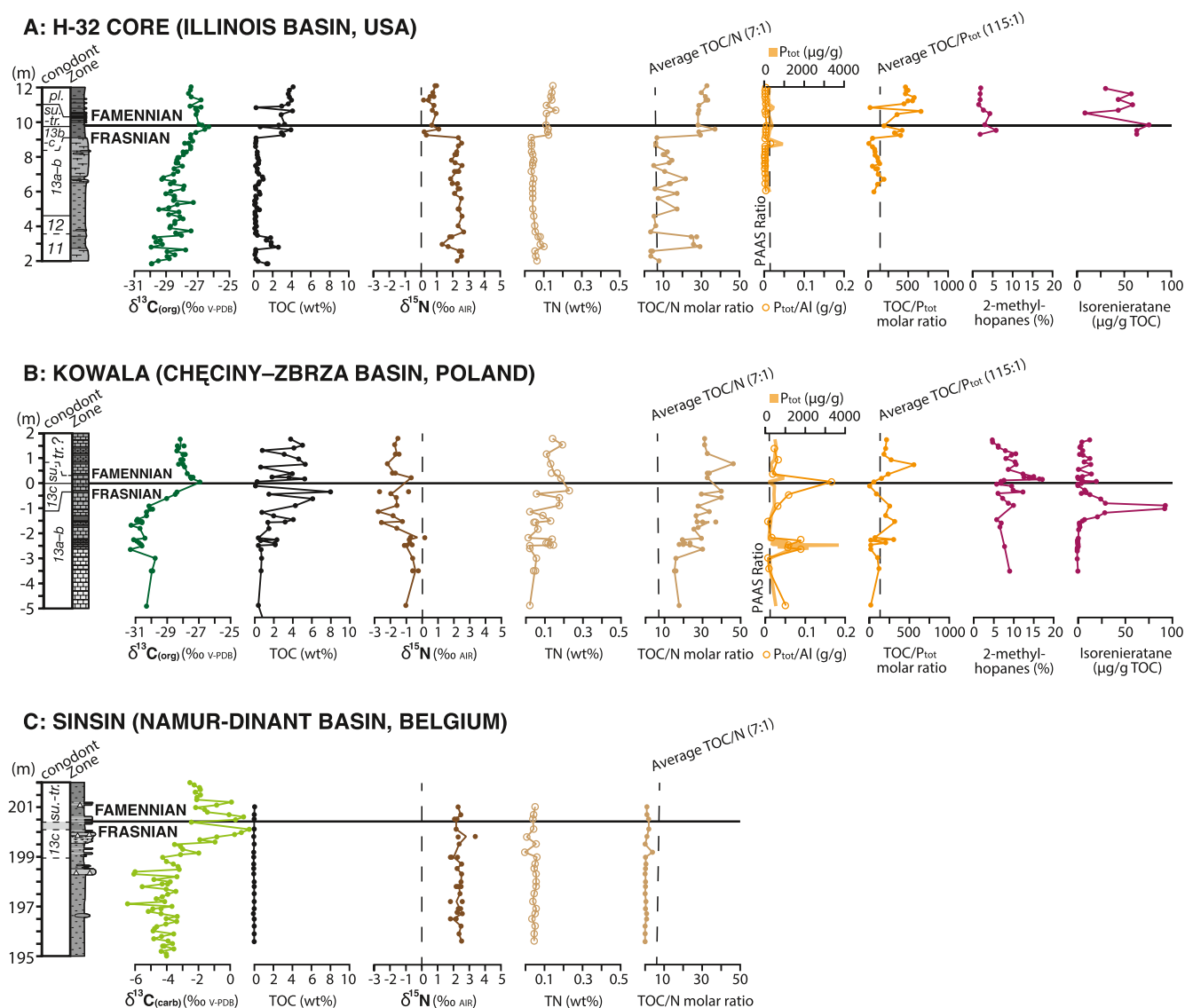


Figure 3. Stratigraphic trends of $\delta^{13}\text{C}$, total organic carbon (TOC), $\delta^{15}\text{N}$, total nitrogen, TOC/N, P_{tot} , P_{tot}/Al , TOC/ P_{tot} , 2-methyl-hopane, and isorenieratane for the H-32 core, Kowala, and Sinsin. All vertical scales are in meters; the stratigraphic position of the FF boundary is indicated for each record. Lithology columns for H-32 and Sinsin are from De Vleeschouwer et al. (2017); for Kowala from Percival et al. (2019). Biostratigraphy for H-32 is from De Vleeschouwer et al. (2017); Kowala from this study (Table S2 in Supporting Information S1); Sinsin from Sandberg et al. (1988), referred to new conodont zonation whereby the presence of *A. ubiquitus* indicates the FZ13c Zone (Girard et al., 2005; Sandberg et al., 2002). Carbon data for the H-32 core are from Liu et al. (2021); Kowala TOC, P_{tot} , and P_{tot}/Al data are from Percival et al. (2019, 2020); Sinsin $\delta^{13}\text{C}$ data are from De Vleeschouwer et al. (2017). All other data are from this study. C/N and C/ P_{tot} Redfield Ratios (Dale et al., 2016), and the Post-Archean average shale P/Al ratio of ~ 0.01 (Taylor & McLennan, 1995), are indicated. Abbreviated conodont zones are: *su.* = *P. subperlobata.*; *tr.* = *P. triangularis.*; *pl.* = *P. del. Platys.*

spanning the FF boundary are more enriched in these biomarkers than the comparatively organic-lean underlying Sweetland Creek sediments, but the low TOC content of the Sweetland Creek rocks hinders biomarker analyses that would confirm this assumption.

5. Discussion

5.1. Potential Diagenetic and Lithological Influences on the $\delta^{15}\text{N}$ Values

High hydrogen index (HI) values and low oxygen index (OI) and T_{max} for both H-32 and Kowala samples indicate that the organic matter in both archives is relatively immature and undegraded (Figure 4). Thus, the effect of organic-matter maturation on $\delta^{15}\text{N}$ values should be minimal for both sites. Early-stage diagenesis has been

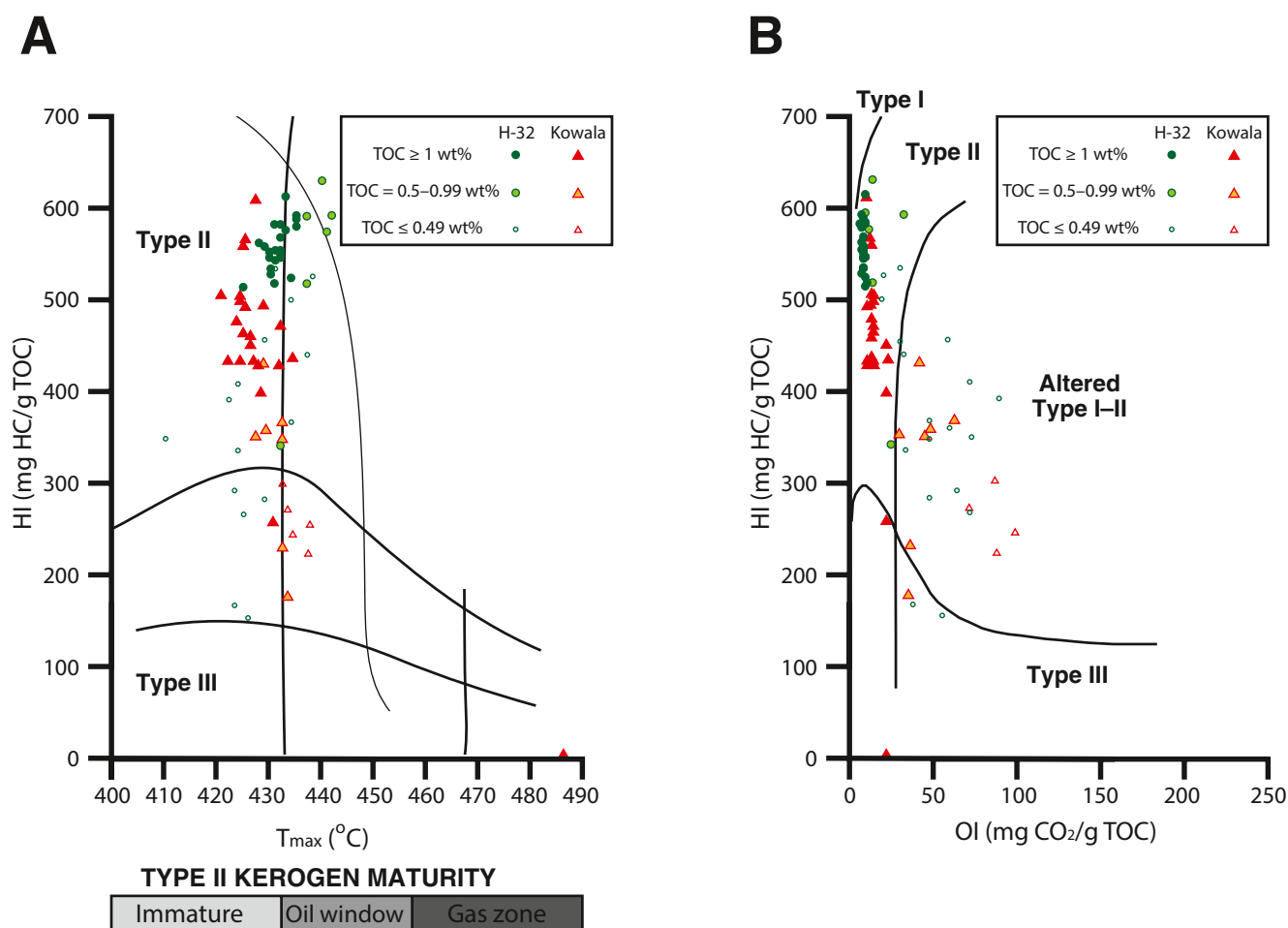


Figure 4. Rock-Eval data for sedimentary rock samples from the H-32 core and Kowala. Kowala data are from Percival et al. (2020); H-32 data are from this study. (a) Hydrogen index (HI) values plotted against the temperature of maximum hydrocarbon generation from kerogen (T_{max}), indicating both the dominant type of kerogen that characterizes the organic matter present in the sample, and its thermal maturity. (b) HI values plotted against oxygen index (OI) values, indicating the type and/or degree of alteration of kerogen that characterizes the organic matter in the sample.

proposed to impact sedimentary nitrogen-isotope compositions, but this would typically cause $\delta^{15}\text{N}$ values to increase, rather than decrease (Freudenthal et al., 2001), contrary to the trends documented in the H-32 and Kowala records. In anoxic conditions such as those hypothesized for the UKW Event, post-depositional decay of microbial matter and addition of bacterial biomass have been reported to cause decreases in $\delta^{15}\text{N}$ values (Lehman et al., 2002). However, this process would require a very large bacterial biomass to affect the $\delta^{15}\text{N}$ values of organic-rich sedimentary rocks (see Junium & Arthur, 2007), which is deemed implausible for the H-32 core and Kowala. Finally, it has been proposed that post-depositional migration of nitrogen (particularly ammonium) can occur between organic-rich and depleted lithologies (e.g., Koehler et al., 2019), but given that this process would be expected to mute or even homogenize a stratigraphic $\delta^{15}\text{N}$ trend, it is not thought to have influenced either the H-32 core or Kowala.

Alternatively, bulk sediment $\delta^{15}\text{N}$ values can be impacted by lithological changes, particularly relating to any input of nitrogen in terrigenous plant/soil material and/or bound to clay minerals as inorganic NH_4^+ , both of which are likely to feature an isotopic composition different to that of fixed nitrogen in seawater. An excellent linear regression in cross-plotted TOC and TN data from the H-32 core ($R^2 = 0.96$; $p < 0.001$) suggests a relatively homogeneous organic-matter composition with a single C/N ratio (Figure 5a; see also Calvert, 2004), likely of marine origin given the dominance of Type II kerogen indicated from the hydrogen index (HI) and oxygen index (OI) data (Figure 4b), and published palynological information from FF records of the Illinois Basin (de la Rue et al., 2007). Whilst the C/N gradient itself (~ 35) is higher than the typical Redfield value of modern

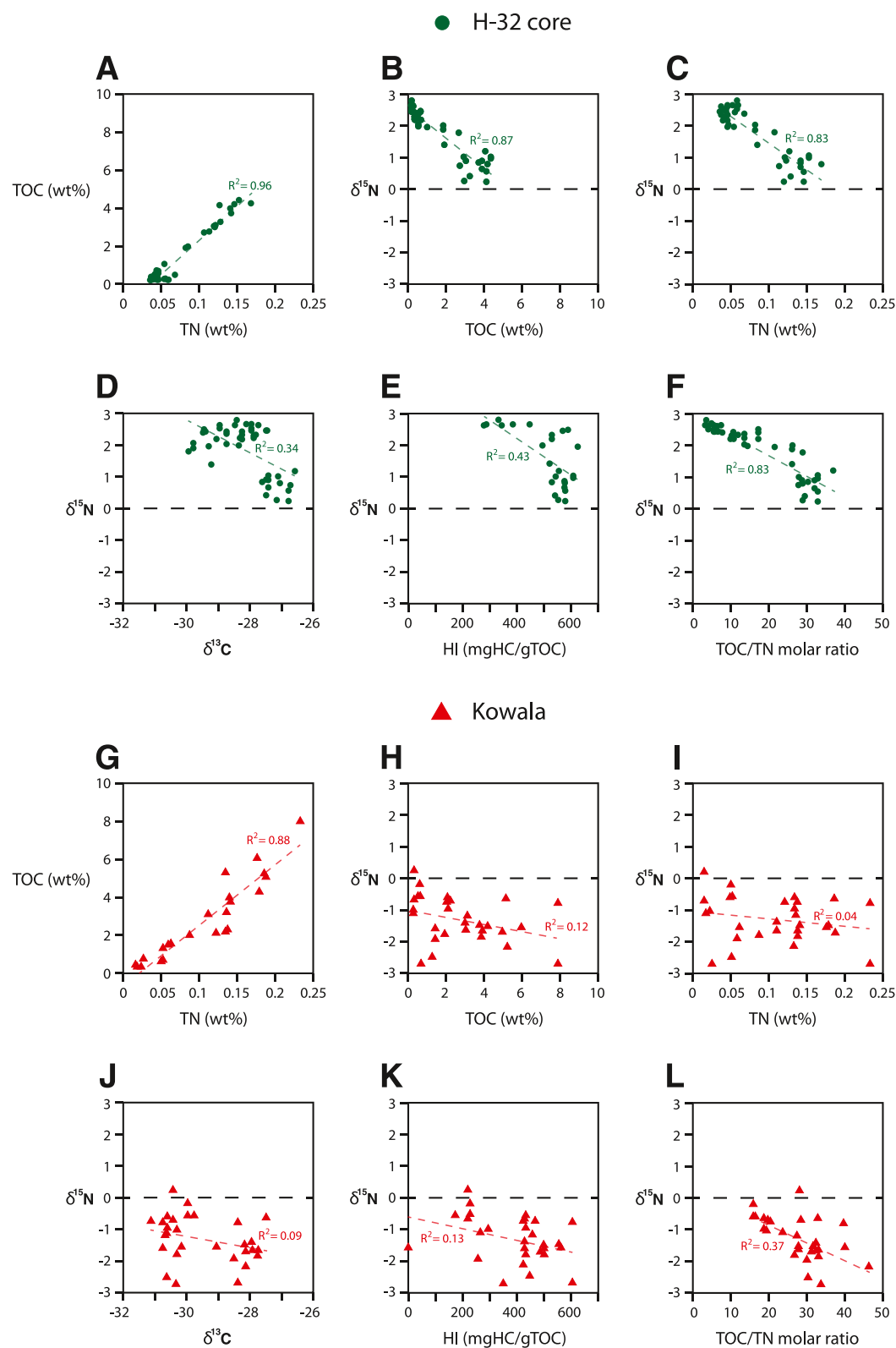


Figure 5. Crossplots of geochemical data from the H-32 core (plots A–F) and Kowala (plots G–L). Data sourced as for Figures 3 and 4.

marine algal material (6–7), it should be noted that an unusually high C/N ratio has previously been documented in several Mesozoic and Paleozoic black shale records featuring primarily marine organic matter (e.g., Algeo et al., 2008; Dumitrescu & Brassell, 2006; Meyers et al., 2006).

However, the distinct *x-intercept* above 0 (~ 0.04 wt% TN; Figure 5a) in the TOC versus TN cross-plot indicates the presence of NH_4^+ in the H-32 sediments, likely as inorganic clay-bound ammonium (see Calvert, 2004). Anaerobic organic-matter degradation has also been proposed as a source of excess NH_4^+ in sediments (Chen et al., 2019), but a similar C/N gradient and *x-intercept* of both TOC-rich and organic-lean samples suggests a consistent NH_4^+ content throughout the studied interval of the H-32 core, which is more supportive of a lithological source given that Al_2O_3 contents are also relatively constant compared to the highly variable TOC levels. Assuming a broadly consistent inorganic NH_4^+ content, the relative proportion of clay-bound nitrogen will be significantly higher in the organic-lean sediments than in the overlying black shales that record the $\delta^{15}\text{N}$ negative excursion, potentially implying that the isotopic shift results solely from that lithological change. Correlations between $\delta^{15}\text{N}$ and both TN and TOC contents further highlight this possibility (Figures 5b and 5c). However, the recorded $\delta^{15}\text{N}$ negative excursion is interpreted to at least partly reflect a true nitrogen-cycle perturbation in the Illinois Basin for several reasons. Firstly, in the organic-lean strata of the Sweetland Creek Shale, TN contents still vary by nearly a factor of 2 (between 0.04 and 0.07 wt%), but show no relationship with $\delta^{15}\text{N}$ values, and there is also no relationship between $\delta^{15}\text{N}$ and TN within the organic-rich sediments of the Grassy Creek Shale. Secondly, the presence of isorenieratane in the black shales is strongly supportive of their deposition under highly reducing conditions, in which some form of nitrogen-cycle perturbation would be expected. Finally, whilst lithological changes can cause a shift in sedimentary $\delta^{15}\text{N}$, an environmental disturbance such as the development of marine anoxia during the FF transition can cause both lithological changes and perturbations to global/local element-cycling geologically simultaneously. This relationship between organic-rich shale deposition and reduction in $\delta^{15}\text{N}$ values has been previously noted for the Illinois Basin (Uveges et al., 2019), and is similar to Mediterranean sapropel records, which are thought to mark a switch from oligotrophic conditions to diazotrophic ones in a more severely reducing water column (Higgins et al., 2010). Thus, it is reasonable to assume that during the FF transition, when marine environments were tending towards more reducing conditions in several regions around the world, the lithological change and $\delta^{15}\text{N}$ excursion recorded in the Illinois Basin were likewise caused by the local manifestation of that environmental degradation (see also e.g., de la Rue et al., 2007; Uveges et al., 2019), rather than the isotopic shift wholly being an artefact of lithological change with no accompanying nitrogen-cycle disturbance.

There is also a small *x-intercept* in the TOC versus TN crossplot for Kowala, but it is less clear than for the H-32 core, with the most organic-lean samples also featuring very low nitrogen contents (<0.05 wt%; Figure 5g). As such, this *x-intercept* may result from data scatter given the weaker linear regression between carbon and nitrogen at this site ($R^2 = 0.88$; $p < 0.001$; Figure 5g), rather than from a significant fraction of inorganic NH_4^+ . The lack of correlation between $\delta^{15}\text{N}$ and either TN or TOC contents (Figures 5h and 5i) supports a minimal lithological influence on the bulk sedimentary nitrogen-isotope composition. However, the aforementioned scatter in the TOC versus TN cross-plot suggests multiple sources of organic matter to the Kowala sediments, implying some input of terrigenous material in addition to marine-derived biomass. HI values below 500 may support such a mixture of bacterial/algal-derived Type II kerogen with terrestrially sourced Type III (Figure 4b), although any terrigenous fraction was likely minor (low HI values due to organic-matter degradation is unlikely given the minimal oxidation/thermal maturity of the sediments indicated by low OI and T_{max} values). Whilst terrestrial organic matter is typically characterized by isotopically lighter carbon and nitrogen compositions, higher C/N ratios, and lower HI values than those of marine biomass (e.g., Schubert & Calvert, 2001; Wada et al., 1987), it is unlikely that the negative nitrogen-isotope excursion at Kowala results solely from an increased deposition of terrigenous material in sediments. Such a control would cause a positive correlation between $\delta^{15}\text{N}$ and both $\delta^{13}\text{C}$ and HI, which is not observed for Kowala (or the H-32 core; Figures 5d, 5e, 5j and 5k). Thus, the $\delta^{15}\text{N}$ trends at Kowala are also interpreted to reflect primary changes to the isotopic composition of seawater, rather than variations in lithology/organic-matter type.

Conversely, it is unlikely that Sinsin records a primary $\delta^{15}\text{N}$ signal. Low TOC and TN contents (<0.1 wt%) and TOC/N molar ratios (mean 1.2) suggest significant organic-matter degradation, and consequent nitrogen loss. This interpretation may be supported further by the lack of a clear positive excursion in $\delta^{13}\text{C}_{(\text{org})}$ at Sinsin like that observed at the FF boundary in other locations (Figure S5 in Supporting Information S1), and is consistent

with previously published evidence for significant post-depositional thermal maturation of sedimentary strata at Sinsin, as well as other Devonian sites in the Belgian Ardennes (Fielitz & Mansy, 1999; Helsen, 1995; Kaiho et al., 2013). Consequently, although the Sinsin $\delta^{15}\text{N}$ values are comparable to background Late Frasnian values reported from several other locations (de la Rue et al., 2007; Levman & Von Bitter, 2002; Uveges et al., 2019; Whalen et al., 2015; *this study*), it is likely that inorganic NH_4^+ comprises most of the nitrogen in the Sinsin rocks, and the site is interpreted as not recording a true seawater composition hereafter.

5.2. Nitrogen Cycling and Perturbations During the Latest Frasnian and the UKW Event

All three investigated sites document background Frasnian $\delta^{15}\text{N}$ values below that of the modern-day average seawater composition ($\sim 4\text{--}5\text{‰}$), consistent with previous studies of Frasnian nitrogen-isotope records (e.g., Levman & Von Bitter, 2002; de la Rue et al., 2007; Whalen et al., 2015; Haddad et al., 2016; Uveges et al., 2019). In the modern, some epicontinental basins, such as the Baltic and Cariaco, can feature seawater $\delta^{15}\text{N}$ values below $4\text{--}5\text{‰}$ (Korth et al., 2014; Thunell et al., 2004; Voss et al., 2005). Thus, the isotopically light nitrogen compositions documented in FF strata from the Illinois and Chęciny–Zbrza basins, which similarly featured reducing water columns and were likely hydrographically restricted to at least some extent, could potentially be explained by their setting. However, background Frasnian sediments between the two Kellwasser horizons, studied from a range of different paleoenvironments, almost invariably feature $\delta^{15}\text{N}$ values between -1 and 3.5‰ (averaging $\sim 1.5\text{‰}$). Thus, the H-32 and Kowala background Frasnian data are consistent with previous models of a warm Late Frasnian–early Famennian marine realm that was more poorly oxygenated, on average, than in the modern (e.g., Joachimski et al., 2009; White et al., 2018). In such an environment, dissolved nitrate levels were likely low, potentially leading to lower levels of water-column denitrification and/or relatively enhanced N fixation compared to today (e.g., Algeo et al., 2014; Kast et al., 2019; Tuite et al., 2019).

The shifts to even lower $\delta^{15}\text{N}$ values in UKW strata recorded in the H-32 and Kowala records may reflect further changes at those two sites during the event, towards a greater influence of N fixation versus denitrification on nitrogen cycling in the water column. This change may have comprised enhanced N fixation, reduced denitrification, or some combination of the two. As noted above, anoxic conditions in modern basinal environments that feature high phosphorus and low nitrate seawater concentrations can promote an increased influence of N fixation on seawater nitrogen isotope compositions relative to levels of denitrification, and consequently low values of seawater $\delta^{15}\text{N}$ (e.g., Cariaco Basin; Thunell et al., 2004). Thus, the documented increases in isorenieratane concentrations and $\text{TOC}/\text{P}_{\text{tot}}$ ratios for the H-32 and Kowala records, indicative of an oxygen-depleted water column enriched in phosphorus where nitrification was stymied and the bioavailable nitrate supply rapidly exhausted, suggest that similar conditions existed in the Illinois and Chęciny–Zbrza basins during the FF transition. Whilst the extent to which the negative $\delta^{15}\text{N}$ excursions resulted from increased N fixation or reduced denitrification (or both) is difficult to determine unambiguously, elevated 2-methyl-hopane concentrations potentially support the former process as playing the key role, as compounds that give rise to this biomarker are produced (albeit not exclusively; Welander et al., 2010) by some diazotrophic cyanobacterial groups today (Summons et al., 1999). Interestingly, this scenario contrasts with previous findings from the Appalachian Basin, where biomarker analyses indicate that low $\delta^{15}\text{N}$ values were likely driven by diminished levels of water-column denitrification, rather than elevated N fixation (Haddad et al., 2016).

However, the $\delta^{15}\text{N}$ values of under -1‰ documented at Kowala are below the lower limit expected from N fixation in the modern, but are comparable with a number of OAE 2 nitrogen-isotope records (e.g., Junium & Arthur, 2007; Jenkyns et al., 2007; Ruvalcaba Baroni et al., 2015). As outlined in Section 1, phytoplanktonic ammonium assimilation has frequently been proposed as the cause of the low OAE 2 $\delta^{15}\text{N}$ values (Higgins et al., 2012). In the context of paleoceanography, the ammonium assimilation model has largely been applied to ocean margin sites where NH_4^+ was sourced from upwelling of oxygen-depleted deep waters (Higgins et al., 2012; Naafs et al., 2019; Ruvalcaba Baroni et al., 2015), although it has also been associated with sapropel formation under highly anoxic (at least intermittently euxinic) conditions in shallower-marine environments of the Peri-Tethys (Junium et al., 2018). Some Pleistocene Mediterranean sapropel horizons also feature very low $\delta^{15}\text{N}$ values (Elling et al., 2021). It should be noted that none of these settings are perfect analogs for the Chęciny–Zbrza Basin during the FF transition, which was situated within a very large carbonate platform area and was at least semi-restricted hydrographically (Percival et al., 2019). However, there is clear evidence for the development of both bottom-water and photic-zone euxinia in the Chęciny–Zbrza Basin during and after the UKW Event, and the

limited understanding of Devonian oceanic circulation (due to paleogeographic and bathymetric uncertainties) means that an influence of upwelling deep waters on this low-latitude region cannot be ruled out. Consequently, whilst further work is needed to establish the exact mechanism that triggered ammonium assimilation, all the pre-requisite conditions for this process could have existed in the Chęciny–Zbrza Basin, with the very low sedimentary $\delta^{15}\text{N}$ values resulting from some combination of it with enhanced nitrogen fixation and/or reduced denitrification. If the highly reducing settings sufficiently depleted seawater molybdenum concentrations, an increased utilisation of Fe- and V-based nitrogenase in N fixation (rather than the typical Mo-based enzyme) might have further lowered $\delta^{15}\text{N}$ values (see Zhang et al., 2014). In addition, given that euxinic conditions also existed (at least intermittently) in the Illinois Basin during the UKW Event, it is possible that ammonium assimilation also played some role in causing the negative $\delta^{15}\text{N}$ excursion at that location. A similar model of decreased denitrification and enhanced ammonium assimilation has been proposed to have promoted marine stress during the Permian–Triassic transition (Sun et al., 2019).

5.3. Variability in the Nature and Timing of Frasnian–Famennian Nitrogen-Cycle Perturbations

Enhanced levels of N fixation and/or reduced water-column denitrification in the Illinois Basin during the UKW Event are consistent with previous interpretations of that area (de la Rue et al., 2007; Uveges et al., 2019). Similar nitrogen-cycle disturbances appear to have occurred across numerous Euramerican epicontinental basins during the UKW Event, documented in the Appalachian Basin (New York, USA; Uveges et al., 2019), and potentially Moose River Basin (Ontario, Canada; Levman & Von Bitter, 2002), although the latter record may be influenced by lithological variations. However, as noted above, these perturbations differed from those in the Chęciny–Zbrza Basin. Additionally, positive $\delta^{15}\text{N}$ excursions recorded at Section C and Fuhe suggest increased importance of water-column denitrification versus N fixation, rather than the other way around, in the Western Canada and Yangshuo basins during the onset of the UKW Event (Whalen et al., 2015; see also Figure S6 in Supporting Information S1). Increased seawater oxygenation during the FF transition has also been proposed for the Yangshuo region (Cui et al., 2021). Furthermore, no major nitrogen-cycle perturbation is documented by sedimentary $\delta^{15}\text{N}$ records in FF boundary strata of the Madre de Dios Basin (Bolivia, Pando X-1 core; Haddad et al., 2016), although this archive is stratigraphically incomplete due to the preservation of thick sandstone units within the studied interval. Clearly, the nature of nitrogen-cycle perturbations associated with the UKW Event varied considerably in different marine settings around the world, consistent with the rapid utilization of fixed nitrogen by marine organisms and consequential short residence time of dissolved nitrogen in seawater.

The Late Devonian cyclostratigraphic timescale developed by De Vleeschouwer et al. (2017), and refined by Da Silva et al. (2020), includes age models based on carbon isotope and magnetic susceptibility variations from all of the H-32 core, Kowala, Section C, and Fuhe. Thus, combining $\delta^{15}\text{N}$ datasets for each site with these age models (Da Silva et al., 2020; De Vleeschouwer et al., 2013, 2017; adapted in the cases of H-32 and Kowala, see Sections 2.1–2.2, and Text S1 in Supporting Information S1) enables production of an absolute timescale for the nitrogen-cycle disturbances in the Illinois, Chęciny–Zbrza, Western Canada, and Yangshuo basins (Figure 6). De Vleeschouwer et al. (2017) determined that the UKW Event commenced ~150 kyr prior to the end of the Frasnian Stage, as marked in the stratigraphic record by the base of the positive $\delta^{13}\text{C}_{\text{carb}}$ excursion. Precisely determining the end of the event is hindered by a lack of stratigraphic consistency in lowermost Famennian carbon-isotope and black-shale records around the world. Consequently, only the nitrogen-cycle perturbations at the onset of the UKW Event in the latest Frasnian are discussed in detail here, as they are easier to compare stratigraphically, and reflect the initiation of environmental changes associated with (and likely at least partly responsible for) the FF mass extinction.

Based on this timescale, enhanced levels of denitrification commenced in Western Canada coeval with the onset of the UKW Event. However, nitrogen-cycle disturbances apparently began later in the Yangshuo and (especially) Illinois basins. Furthermore, the nitrogen-cycle perturbation in the Chęciny–Zbrza basin took place 94 kyr prior to the onset of enhanced carbon burial that characterized the UKW Event. The geographic asynchronicity of these nitrogen-cycle disturbances is consistent with the stratigraphic position of the $\delta^{15}\text{N}$ excursion relative to the base of the positive $\delta^{13}\text{C}$ shift in each of the four records (Figure S6 in Supporting Information S1).

Uranium-isotope trends reported by Song et al. (2017) indicate a gradual transition towards increasingly widespread oxygen-depleted conditions throughout the global ocean ~250–350 kyr prior to the onset of the UKW Event (based on assumed sedimentation rates for their record), supporting an early development of redox-induced

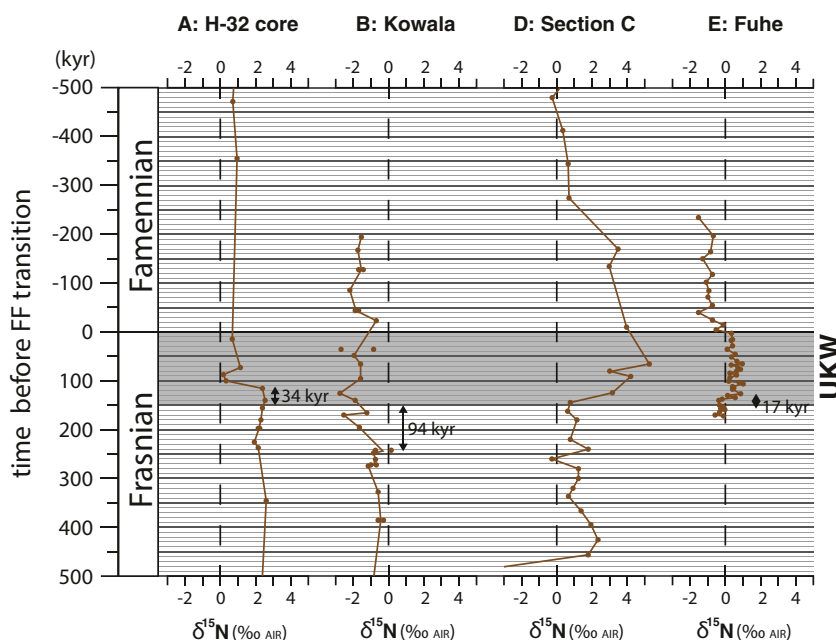


Figure 6. Stratigraphic $\delta^{15}\text{N}$ trends for Frasnian–Famennian (FF) archives studied here and by Whalen et al. (2015), plotted with respect to time in kyr before the FF transition. The thin black line indicates the FF boundary; the shaded gray area marks the timing of the early part of the Upper Kellwasser (UKW) Event prior to the end of the Frasnian Stage (De Vleeschouwer et al., 2017). For the H-32 core, Kowala, and Fuhe, the estimated time in kyr between the onset of local nitrogen-cycle disturbance and the global carbon-cycle perturbation is indicated, based on the cyclostratigraphic age models for each record (De Vleeschouwer et al., 2013, 2017; Da Silva et al., 2020; *this study*).

nitrogen-cycle perturbations in some shelf environments, such as the Chęciny–Zbrza Basin. Given that the black shales and positive $\delta^{13}\text{C}$ excursion characteristic of UKW strata are assumed to have resulted from widespread organic-matter burial under anoxic conditions, the commencement of marine anoxia prior to the UKW Event *sensu stricto* is expected, and the same sequence of events has been demonstrated for OAE 2 (Ostrander et al., 2017). However, White et al. (2018) suggested that global-scale anoxia was most prevalent earlier in the Frasnian, and that the open-ocean became more oxygenated immediately prior to the UKW Event. Further work is needed to resolve how anoxic conditions developed in the open ocean during the latest Frasnian, potentially via investigation of oceanic-island records such as Boulongour Reservoir (Xinjiang, NW China; Carmichael et al., 2014).

5.4. Implications for the Global Environmental Changes Associated With the UKW Event

The asynchronous onset of nitrogen-cycle disturbances recorded from the Illinois and Chęciny–Zbrza basins highlights the importance of local controls on such perturbations, and further emphasizes the key role of terrigenous nutrient runoff from enhanced continental weathering in driving environmental degradation during the UKW Event. Previous studies have highlighted a major influx of terrigenous nutrients to the marine realm during the FF transition, and particularly an increase in phosphorus at several sites around the world (Carmichael et al., 2014; Percival et al., 2020; Sageman et al., 2003). At Kowala, this large influx of non-detrital phosphorus is recorded by peaks in P_{tot} and P_{tot}/Al in uppermost Frasnian strata (Figure 3b; see also Percival et al., 2020). An external influx of the phosphorus, rather than enhanced scavenging and deposition, is confirmed by the lack of stratigraphic correlation between the P_{tot} and P_{tot}/Al peaks and other element contents or redox proxies (Figure 3b). However, the stratigraphic position of phosphorus enrichment just below documented excursions in $\delta^{15}\text{N}$, isorenieratane, and $\text{TOC}/P_{\text{tot}}$ is consistent with an enhanced supply of this major nutrient in the Chęciny–Zbrza Basin triggering localized marine anoxia–euxinia just prior to the onset of the global carbon-cycle perturbation (Figure 3b; see also Percival et al., 2020).

By contrast, the absence of such a clear peak in P_{tot} or P_{tot}/Al values in Frasnian–Famennian strata of the H-32 core indicates minimal change in the influx of this macronutrient to the Illinois Basin at the onset of the UKW

Event (Figure 3a). Interestingly, a lack of increased phosphorus influx to the Illinois Basin during the FF transition contrasts with previous hypotheses of terrigenous nutrient runoff as the driver of anoxic–euxinic conditions in that setting (see Uveges et al., 2019). Nonetheless, given the delayed development of oxygen-depleted conditions in the Illinois Basin compared to the Chęciny-Zbrza region, this pattern ultimately supports global-scale enhanced runoff of nutrients such as phosphorus as the initial trigger of marine anoxia–euxinia in regions where it commenced earliest, prior to the UKW Event *sensu stricto*. In areas that lacked such a rise in direct phosphorus input, environmental degradation may have been relatively minor unless/until stimulation via a different trigger or through the migration/expansion of oxygen-depleted water masses formed elsewhere. Whilst a non-terrestrial source of phosphorus cannot be excluded as the driver of widespread marine anoxia during the UKW Event, the peaks in P_{tot} and P_{tot}/Al at Kowala broadly correlates with a radiogenic shift in osmium-isotope ratios indicative of globally enhanced continental weathering (Percival et al., 2020). The presence or absence of terrestrially-derived phosphorus in determining when anoxic–euxinic conditions developed in the Illinois and Chęciny-Zbrza basins is further supported by the greater evidence of terrigenous organic matter at Kowala compared to the H-32 core (see Figure 4 and Section 5.1).

Intriguingly, whilst geographically variable nitrogen-cycle disturbances would be expected during a major climate-change event, this pattern stands in contrast to shallow marine records of the Mesozoic OAEs. All studied epicontinental basin archives of OAE 2 show a negative excursion generally interpreted as marking increased N fixation (Danzelle et al., 2020; Ruvalcaba Baroni et al., 2015; Zhang et al., 2019). In contrast, shallow-marine records of the Toarcian OAE invariably record positive excursions suggestive of enhanced denitrification (Jenkyns et al., 2001; Kemp et al., 2019). It is possible that shallow-marine environments during each of the Toarcian OAE and OAE 2 featured N-cycle disturbances that were as locally variable as during the Devonian, but that their existing $\delta^{15}\text{N}$ records are affected by sampling bias. Alternatively, the different UKW and Mesozoic $\delta^{15}\text{N}$ patterns may highlight greater geographic variability in environmental degradation during the Paleozoic crisis, due to the different type of climate change and/or nutrient source associated with this earlier event. The Mesozoic OAEs were generally marked by significant climate warming (albeit occasionally featuring transient cooling/reoxygenation pulses) and, during OAE 2, significant submarine micronutrient release in addition to terrigenous runoff, both of which would have promoted marine stratification and anoxia globally (Robinson et al., 2017). By contrast, the global cooling that prevailed during the UKW Event should have stymied water-column deoxygenation; nor is there evidence of a submarine volcanic plateau that could have released micronutrients directly to the ocean. Consequently, nutrient cycling and the development of marine anoxia were likely more dependent on local–regional processes such as terrigenous runoff and consequent eutrophication (i.e., the ‘top down’ model summarized in Carmichael et al., 2019). The importance of diachronous local–regional terrestrial processes in triggering marine anoxia during the UKW Event may highlight a key role for mountain formation and/or land-plant expansion in causing the environmental perturbations associated with the FF extinction (see Algeo et al., 1995; Averbuch et al., 2005). However, it is also possible that the anoxia was associated with enhanced weathering and riverine runoff caused by a global-scale trigger that simply impacted different geographic regions variably and diachronously. Interestingly, some earlier Paleozoic major carbon-burial events also coincided with global cooling and widespread marine anoxia (e.g., the end-Ordovician mass extinction; Bartlett et al., 2018). Thus, local processes may have been similarly crucial in stimulating marine anoxia during those crises, leading to comparable variations in the onset and severity of environmental degradation in different settings across the globe.

6. Conclusions

This study documents negative $\delta^{15}\text{N}$ excursions in the H-32 core and Kowala Quarry archives of the Frasnian–Famennian interval, together with consistent (but probably not primary) values at Sinsin. Detection of 2-methylhopanes and isorenieratane, as well as high $\text{TOC}/P_{\text{tot}}$ ratios, in H-32 and Kowala strata correlative with the $\delta^{15}\text{N}$ shifts supports the development of euxinic conditions that resulted in an enhanced N fixation and/or reduced water-column denitrification influence on local nitrogen cycling. Very low $\delta^{15}\text{N}$ values at Kowala likely indicate phytoplanktonic ammonium assimilation under extremely reducing conditions, possibly coupled with the utilisation of atypical Fe- and/or V-based nitrogenases for N fixation. Cyclostratigraphic correlation of the H-32 and Kowala trends with records from Western Canada and South China highlight that whilst Frasnian–Famennian environmental perturbations took place on a global scale, they were regionally variable in terms of their nature

and timing, with >100 kyr separating the onset of changes across those individual areas. The earliest environmental degradation is recorded at Kowala, coeval with a major input of terrestrially sourced phosphorus to that setting; by contrast, the H-32 core documents a later onset of marine anoxia and no such nutrient influx. These findings re-emphasize the importance of terrestrial nutrient runoff in initiating global environmental degradation during the Frasnian–Famennian transition, and demonstrate its key role in determining when those changes began, and how they were locally manifested.

Data Availability Statement

The geochemical and age-model data are available in the repository PANGAEA (<https://doi.org/10.1594/PANGAEA.943316>).

Acknowledgments

We thank Thomas Algeo, Eva Stüeken, and further anonymous reviewers for feedback that has improved this manuscript. We greatly appreciate lab assistance from David Verstraeten, Kaidi Wang, and Delphine Vandeputte, and also thank Christophe Snoeck and Yadong Sun for helpful discussions regarding nitrogen analyses, Gilbert Klapper for remarks on conodont taxonomy and biostratigraphy pertaining to the Kowala record, and Jed Day and the Iowa Geological Survey for access to and biostratigraphic information on the H-32 core. We thank the Research Foundation—Flanders (FWO: grant 12P4519N to LMEP and Hercules Middle size Instrument funding), Vrije Universiteit Brussel Strategic Research (PC), Scientific Research Fund (FNRS, grant C 60/5—CDR/OL) and International Geoscience Program (Project 652: Reading Geologic time in Paleozoic sedimentary rocks) to ACDS, the National Science Centre—Poland (MAESTRO grants 2013/08/A/ST10/00717 and 2014/15/B/ST10/03705 including LM and MR), and the Polish Geological Institute—National Research Institute (PGI-NRI project number 62.9012.1903.00.0) to KN for funding.

References

- Algeo, T., Rowe, H., Hower, J. C., Schwark, L., Herrmann, A., & Heckel, P. (2008). Changes in ocean denitrification during Late Carboniferous glacial–interglacial cycles. *Nature Geoscience*, 1(10), 709–714. <https://doi.org/10.1038/ngeo307>
- Algeo, T. J., Berner, R. A., Maynard, J. B., & Scheckler, S. E. (1995). Late Devonian oceanic anoxic events and biotic crises: “rooted” in the evolution of vascular land plants. *Geological Society of America Today*, 5, 45–66.
- Algeo, T. J., Lyons, T. W., Blakey, R. C., & Over, D. J. (2007). Hydrographic conditions of the Devonian–Carboniferous North American Seaway inferred from sedimentary Mo–TOC relationships. *Palaeogeography, Palaeoclimatology, Palaeoecology*, 256(3–4), 204–230. <https://doi.org/10.1016/j.palaeo.2007.02.035>
- Algeo, T. J., Meyers, P. A., Robinson, R. S., Rowe, H., & Jiang, G. Q. (2014). Icehouse–greenhouse variations in marine denitrification. *Biogeosciences*, 11(4), 1273–1295. <https://doi.org/10.5194/bg-11-1273-2014>
- Algeo, T. J., & Tribouillard, N. (2009). Environmental analysis of paleoceanographic systems based on molybdenum–uranium covariation. *Chemical Geology*, 268(3–4), 211–225. <https://doi.org/10.1016/j.chemgeo.2009.09.001>
- Altabet, M. A. (2007). Constraints on oceanic N balance/imbalance from sedimentary ¹⁵N records. *Biogeosciences*, 4(1), 75–86. <https://doi.org/10.5194/bg-4-75-2007>
- Averbuch, O., Tribouillard, N., Devleeschouwer, X., Riquier, L., Mistiaen, B., & Vliet-Lanoe, V. (2005). Mountain building-enhanced continental weathering and organic carbon burial as major causes for climatic cooling at the Frasnian–Famennian boundary (c. 376 Ma)? *Terra Nova*, 17(1), 25–34. <https://doi.org/10.1111/j.1365-3121.2004.00580.x>
- Balter, V., Renaud, S., Girard, C., & Joachimski, M. M. (2008). Record of climate-driven morphological changes in 376 Ma Devonian fossils. *Geology*, 36(11), 907–910. <https://doi.org/10.1130/G24989A.1>
- Bartlett, R., Elrick, M., Wheeley, J. R., Polyak, V., Desrochers, A., & Asmerom, Y. (2018). Abrupt global-ocean anoxia during the Late Ordovician–early Silurian detected using uranium isotopes of marine carbonates. *Proceedings of the National Academy of Sciences*, 115(23), 5896–5901. <https://doi.org/10.1073/pnas.1802438115>
- Behar, F., Beaumont, V., de, B., & Penteado, H. L. (2001). Rock-Eval 6 technology: Performances and developments. *Oil and Gas Science and Technology*, 56(2), 111–134. <https://doi.org/10.2516/ogst:2001013>
- Bond, D. P., & Grasby, S. E. (2017). On the causes of mass extinctions. *Palaeogeography, Palaeoclimatology, Palaeoecology*, 478, 3–29. <https://doi.org/10.1016/j.palaeo.2016.11.005>
- Bond, D. P. G., Wignall, P. B., & Racki, G. (2004). Extent and duration of marine anoxia during the Frasnian–Famennian (Late Devonian) mass extinction in Poland, Germany, Austria and France. *Geological Magazine*, 141(2), 173–193. <https://doi.org/10.1017/S0016756804008866>
- Bond, D. P. G., & Zatoń, M. (2003). Gamma-ray spectrometry across the Upper Devonian basin succession at Kowala in the Holy Cross Mountains (Poland). *Acta Geologica Polonica*, 53, 93–99.
- Calvert, S. E. (2004). Beware intercepts: Interpreting compositional ratios in multi-component sediments and sedimentary rocks. *Organic Geochemistry*, 35(8), 981–987. <https://doi.org/10.1016/j.orggeochem.2004.03.001>
- Carmichael, S. K., Waters, J. A., Königshof, P., Suttner, T. J., & Kido, E. (2019). Paleogeography and paleoenvironments of the Late Devonian Kellwasser event: A review of its sedimentological and geochemical expression. *Global and Planetary Change*, 183, 102984. <https://doi.org/10.1016/j.gloplacha.2019.102984>
- Carmichael, S. K., Waters, J. A., Suttner, T. J., Kido, E., & DeReuil, A. A. (2014). A new model for the Kellwasser Anoxia Events (Late Devonian): Shallow water anoxia in an open oceanic setting in the Central Asian Orogenic Belt. *Palaeogeography, Palaeoclimatology, Palaeoecology*, 399, 394–403. <https://doi.org/10.1016/j.palaeo.2014.02.016>
- Casier, J. G. (2017). Ecology of Devonian ostracods: Application to the Frasnian/Famennian boundary bioevent in the type region (Dinant Synclinorium, Belgium). *Palaeobiodiversity and Palaeoenvironments*, 97(3), 553–564. <https://doi.org/10.1007/s12549-017-0278-z>
- Casier, J. G., & Devleeschouwer, X. (1995). *Arguments (ostracodes) pour une régression culminant à proximité de la limite Frasnien–Famennien à Sinsin* (Vol. 65, p. 51–68). Bulletin de l’Institut Royal des Sciences Naturelles de Belgique: Sciences de la Terre.
- Chen, Y., Diamond, C. W., Stüeken, E. E., Cai, C., Gill, B. C., Zhang, F., et al. (2019). Coupled evolution of nitrogen cycling and redoxcline dynamics on the Yangtze Block across the Ediacaran–Cambrian transition. *Geochimica et Cosmochimica Acta*, 257, 243–265. <https://doi.org/10.1016/j.gca.2019.05.017>
- Claeys, P., Kyte, F. T., Herbolch, A., & Casier, J. G. (1996). Geochemistry of the Frasnian–Famennian boundary in Belgium: Mass extinction, anoxic oceans and microtektite layer, but not much iridium? *Geological Society of America Special Paper*, 307, 491–504. <https://doi.org/10.1130/0-8137-2307-8.491>
- Clifford, D. J., Clayton, J. L., & Sinninghe Damsté, J. S. (1998). 2,3,6-/3,4,5-Trimethyl substituted diaryl carotenoid derivatives (Chlorobiaceae) in petroleum of the Belarussian Pripyat River Basin. *Organic Geochemistry*, 29(5–7), 1253–1267. [https://doi.org/10.1016/S0146-6380\(98\)00086-2](https://doi.org/10.1016/S0146-6380(98)00086-2)
- Cui, Y., Shen, B., Sun, Y., Ma, H., Chang, J., Li, F., et al. (2021). A pulse of seafloor oxygenation at the Late Devonian Frasnian–Famennian boundary in South China. *Earth-Science Reviews*, 218, 103651. <https://doi.org/10.1016/j.earscirev.2021.103651>

- Dale, A. W., Boyle, R. A., Lenton, T. M., Ingall, E. D., & Wallmann, K. (2016). A model for microbial phosphorus cycling in bioturbated marine sediments: Significance for phosphorus burial in the early Paleozoic. *Geochimica et Cosmochimica Acta*, 189, 251–268. <https://doi.org/10.1016/j.gca.2016.05.046>
- Danzelle, J., Riquier, L., Baudin, F., Thomazo, C., & Puc  at, E. (2020). Nitrogen and carbon cycle perturbations through the Cenomanian-Turonian oceanic anoxic event 2 (~94 Ma) in the Vocontian Basin (SE France). *Palaeogeography, Palaeoclimatology, Palaeoecology*, 538, 109443. <https://doi.org/10.1016/j.palaeo.2019.109443>
- Da Silva, A. C., Sinnesael, M., Claeys, P., Davies, J. H. F. L., deWinter, N. J., Percival, L. M. E., et al. (2020). Anchoring the Late Devonian mass extinction in absolute time by integrating climatic controls and radio-isotopic dating. *Scientific Reports*, 10(1), 12940. <https://doi.org/10.1038/s41598-020-69097-6>
- Day, J., & Witzke, B. J. (2017). Upper Devonian biostratigraphy, event stratigraphy, and Late Frasnian Kellwasser extinction bioevents in the Iowa Basin: Western Euramerica. In M. Montanari (Ed.), *Stratigraphy & Timescales* (Vol. 2, p. 243–332). <https://doi.org/10.1016/bs.sats.2017.08.002>
- de la Rue, S. R., Rowe, H. D., & Rimmer, S. M. (2007). Palynological and bulk geochemical constraints on the paleoceanographic conditions across the Frasnian–Famennian boundary, New Albany Shale, Indiana. *International Journal of Coal Geology*, 71(1), 72–84. <https://doi.org/10.1016/j.coal.2006.06.003>
- De Vleeschouwer, D., Da Silva, A. C., Sinnesael, M., Chen, D., Day, J. E., Whalen, M. T., et al. (2017). Timing and pacing of the Late Devonian mass extinction event regulated by eccentricity and obliquity. *Nature Communications*, 8(1), 1–11. <https://doi.org/10.1038/s41467-017-02407-1>
- De Vleeschouwer, D., Rakoci  ski, M., Racki, G., Bond, D. P. G., Sobie  , K., & Claeys, P. (2013). The astronomical rhythm of Late-Devonian climate change (Kowala section, Holy Cross Mountains, Poland). *Earth and Planetary Science Letters*, 365, 25–37. <https://doi.org/10.1016/j.epsl.2013.01.016>
- Dumitrescu, M., & Brassell, S. C. (2006). Compositional and isotopic characteristics of organic matter for the early Aptian Oceanic Anoxic Event at Shatsky Rise, ODP Leg 198. *Palaeogeography, Palaeoclimatology, Palaeoecology*, 235(1–3), 168–191. <https://doi.org/10.1016/j.palaeo.2005.09.028>
- Elling, F. J., Hemingway, J. D., Kharbush, J. J., Becker, K. W., Polik, C. A., & Pearson, A. (2021). Linking diatom-diazotroph symbioses to nitrogen cycle perturbations and deep-water anoxia: Insights from Mediterranean sapropel events. *Earth and Planetary Science Letters*, 571, 117110. <https://doi.org/10.1016/j.epsl.2021.117110>
- Espitali  , J., Deroo, G., & Marquis, F. (1985). Rock-Eval Pyrolysis and its Applications. *Revue de l'Institut Fran  ais du P  trole*, 40(5), 563–579. <https://doi.org/10.2516/ogst:1985035>
- Fielitz, W., & Mansy, J. L. (1999). Pre-and synorogenic burial metamorphism in the Ardenne and neighbouring areas (Rhenohercynian zone, central European Variscides). *Tectonophysics*, 309(1–4), 227–256. [https://doi.org/10.1016/S0040-1951\(99\)00141-9](https://doi.org/10.1016/S0040-1951(99)00141-9)
- Freudenthal, T., Wagner, T., Wenzh  fer, F., Zabel, M., & Wefer, G. (2001). Early diagenesis of organic matter from sediments of the eastern subtropical Atlantic: Evidence from stable nitrogen and carbon isotopes. *Geochimica et Cosmochimica Acta*, 65(11), 1795–1808. [https://doi.org/10.1016/S0016-7037\(01\)00554-3](https://doi.org/10.1016/S0016-7037(01)00554-3)
- Girard, C., Klapper, G., & Feist, R. (2005). Subdivision of the terminal Frasnian linguiformis conodont Zone, revision of the correlative interval of Montagne Noire Zone 13, and discussion of stratigraphically significant associated trilobites. In D. J. Over, J. R. Morrow, & P. B. Wignall, (Eds.), *Understanding Late Devonian and Permian-Triassic Biotic and Climatic Events: Towards an Integrated Approach. Developments in Palaeontology and Stratigraphy* (Vol. 20, p. 181–198). [https://doi.org/10.1016/S0920-5446\(05\)80007-X](https://doi.org/10.1016/S0920-5446(05)80007-X)
- Grice, K., Schaeffer, P., Schwark, L., & Maxwell, J. R. (1997). Changes in palaeoenvironmental conditions during deposition of the Permian Kupferschiefer (Lower Rhine Basin, northwest Germany) inferred from molecular and isotopic compositions of biomarker components. *Organic Geochemistry*, 26(11–12), 677–690. [https://doi.org/10.1016/S0146-6380\(97\)00036-3](https://doi.org/10.1016/S0146-6380(97)00036-3)
- Haddad, E. E., Tuite, M. L., Martinez, A. M., Williford, K., Boyer, D. L., Droser, M. L., & Love, G. D. (2016). Lipid biomarker stratigraphic records through the Late Devonian Frasnian/Famennian boundary: Comparison of high- and low-latitude epicontinental marine settings. *Organic Geochemistry*, 98, 38–53. <https://doi.org/10.1016/j.orggeochem.2016.05.007>
- Helsen, S. (1995). Burial history of Palaeozoic strata in Belgium as revealed by conodont colour alteration data and thickness distributions. *Geologische Rundschau*, 84(4), 738–747. <https://doi.org/10.1007/BF00240564>
- Higgins, M. B., Robinson, R. S., Carter, S. J., & Pearson, A. (2010). Evidence from chlorin nitrogen isotopes for alternating nutrient regimes in the Eastern Mediterranean Sea. *Earth and Planetary Science Letters*, 290(1–2), 102–107. <https://doi.org/10.1016/j.epsl.2009.12.009>
- Higgins, M. B., Robinson, R. S., Husson, J. M., Carter, S. J., & Pearson, A. (2012). Dominant eukaryotic export production during ocean anoxic events reflects the importance of recycled NH₄⁺. *Proceedings of the National Academy of Sciences of the United States of America*, 109(7), 2269–2274. <https://doi.org/10.1073/pnas.1104313109>
- Jenkyns, H. C. (2010). Geochemistry of oceanic anoxic events. *Geochemistry, Geophysics, Geosystems*, 11(3), Q03004. <https://doi.org/10.1029/2009GC002788>
- Jenkyns, H. C., Gr  cke, D. R., & Hesselbo, S. P. (2001). Nitrogen isotope evidence for water mass denitrification during the early Toarcian (Jurassic) oceanic anoxic event. *Paleoceanography*, 16(6), 593–603. <https://doi.org/10.1029/2000PA000558>
- Jenkyns, H. C., Matthews, A., Tsikos, H., & Erel, Y. (2007). Nitrate reduction, sulfate reduction, and sedimentary iron isotope evolution during the Cenomanian-Turonian oceanic anoxic event. *Paleoceanography*, 22(3), PA3208. <https://doi.org/10.1029/2006PA001355>
- Joachimski, M. M., Breisig, S., Buggisch, W., Talent, J. A., Mawson, R., Gereke, M., et al. (2009). Devonian climate and reef evolution: Insights from oxygen isotopes in apatite. *Earth and Planetary Science Letters*, 284(3–4), 599–609. <https://doi.org/10.1016/j.epsl.2009.05.028>
- Joachimski, M. M., & Buggisch, W. (2002). Conodont apatite $\delta^{18}\text{O}$ signatures indicate climatic cooling as a trigger of the Late Devonian mass extinction. *Geology*, 30(8), 711–714. [https://doi.org/10.1130/0091-7613\(2002\)030<0711:CAOSIC>2.0.CO;2](https://doi.org/10.1130/0091-7613(2002)030<0711:CAOSIC>2.0.CO;2)
- Joachimski, M. M., Ostertag-Henning, C., Pancost, R. D., Strauss, H., Freeman, K. H., Littke, R., et al. (2001). Water column anoxia, enhanced productivity and concomitant changes in $\delta^{13}\text{C}$ and $\delta^{34}\text{S}$ across the Frasnian–Famennian boundary (Kowala—Holy Cross Mountains/Poland). *Chemical Geology*, 175(1–2), 109–131. [https://doi.org/10.1016/S0009-2541\(00\)00365-X](https://doi.org/10.1016/S0009-2541(00)00365-X)
- Joachimski, M. M., Pancost, R. D., Freeman, K. H., Ostertag-Henning, C., & Buggisch, W. (2002). Carbon isotope geochemistry of the Frasnian–Famennian transition. *Palaeogeography, Palaeoclimatology, Palaeoecology*, 181(1–3), 91–109. [https://doi.org/10.1016/S0031-0182\(01\)00474-6](https://doi.org/10.1016/S0031-0182(01)00474-6)
- Junium, C. K., & Arthur, M. A. (2007). Nitrogen cycling during the Cretaceous, Cenomanian-Turonian oceanic anoxic event II. *Geochemistry, Geophysics, Geosystems*, 8(3), Q03002. <https://doi.org/10.1029/2006GC003128>
- Junium, C. K., Dickson, A. J., & Uveges, B. T. (2018). Perturbation to the nitrogen cycle during rapid Early Eocene global warming. *Nature Communications*, 9(1), 3186. <https://doi.org/10.1038/s41467-018-05486-w>
- Kaiho, K., Yatsu, S., Oba, M., Gorjan, P., Casier, J. G., & Ikeda, M. (2013). A forest fire and soil erosion event during the Late Devonian mass extinction. *Palaeogeography, Palaeoclimatology, Palaeoecology*, 392, 272–280. <https://doi.org/10.1016/j.palaeo.2013.09.008>

- Kast, E. R., Stolper, D. A., Auderset, A., Higgins, J. A., Ren, H., Wang, X. T., et al. (2019). Nitrogen isotope evidence for expanded ocean suboxia in the early Cenozoic. *Science*, 364(6438), 386–389. <https://doi.org/10.1126/science.aau5784>
- Kemp, D. B., Baranyi, V., Izumi, K., & Burgess, R. D. (2019). Organic matter variations and links to climate across the early Toarcian oceanic anoxic event (T-OAE) in Toyora area, southwest Japan. *Palaeogeography, Palaeoclimatology, Palaeoecology*, 530, 90–102. <https://doi.org/10.1016/j.palaeo.2019.05.040>
- Klapper, G., & Kirchgasser, W. T. (2016). Frasnian Late Devonian conodont biostratigraphy in New York: Graphic correlation and taxonomy. *Journal of Paleontology*, 90(3), 525–554. <https://doi.org/10.1017/jpa.2015.70>
- Koehler, M. C., Stüeken, E. E., Hillier, S., & Prave, A. R. (2019). Limitation of fixed nitrogen and deepening of the carbonate-compensation depth through the Hirnantian at Dob's Linn, Scotland. *Palaeogeography, Palaeoclimatology, Palaeoecology*, 534, 109321. <https://doi.org/10.1016/j.palaeo.2019.109321>
- Koopmans, M. P., Köster, J., VanKaam-Peters, H. M. E., Kenig, F., Schouten, S., Hartgers, W. A., et al. (1996). Diagenetic and catagenetic products of isorenieratene: Molecular indicators for photic zone anoxia. *Geochimica et Cosmochimica Acta*, 60(22), 4467–4496. [https://doi.org/10.1016/S0016-7037\(96\)00238-4](https://doi.org/10.1016/S0016-7037(96)00238-4)
- Korth, F., Deutsch, B., Frey, C., Moros, C., & Voss, M. (2014). Nitrate source identification in the Baltic Sea using its isotopic ratios in combination with a Bayesian isotope mixing model. *Biogeochemistry*, 11(17), 4913–4924. <https://doi.org/10.5194/bg-11-4913-2014>
- Lehmann, M. F., Bernasconi, S. M., Barbieri, A., & McKenzie, J. A. (2002). Preservation of organic matter and alteration of its carbon and nitrogen isotope composition during simulated and in situ early sedimentary diagenesis. *Geochimica et Cosmochimica Acta*, 66(20), 3573–3584. [https://doi.org/10.1016/S0016-7037\(02\)00968-7](https://doi.org/10.1016/S0016-7037(02)00968-7)
- Levman, B. G., & Von Bitter, P. H. (2002). The Frasnian–Famennian (mid-Late Devonian) boundary in the type section of the Long Rapids Formation, James Bay Lowlands, northern Ontario, Canada. *Canadian Journal of Earth Sciences*, 39(12), 1795–1818. <https://doi.org/10.1139/e02-073>
- Liu, Z., Percival, L. M. E., VanDerputte, D., Selby, D., Claeys, P., Over, D. J., & Gao, Y. (2021). Late Devonian mercury record from North America and its implications for the Frasnian–Famennian mass extinction. *Palaeogeography, Palaeoclimatology, Palaeoecology*, 576, 110502. <https://doi.org/10.1016/j.palaeo.2021.110502>
- Marconi, D., Sigman, D. M., Casciotti, K. L., Campbell, E. C., Weigand, M. A., Fawcett, S. E., et al. (2017). Tropical Dominance of N₂ Fixation in the North Atlantic Ocean. *Global Biogeochemical Cycles*, 31(10), 1608–1623. <https://doi.org/10.1002/2016GB005613>
- Marynowski, L., Rakociński, M., Boruch, E., Kremer, B., Schubert, B. A., & Jähren, A. H. (2011). Molecular and petrographic indicators of redox conditions and bacterial communities after the F/F mass extinction (Kowala, Holy Cross Mountains, Poland). *Palaeogeography, Palaeoclimatology, Palaeoecology*, 306(1–2), 1–14. <https://doi.org/10.1016/j.palaeo.2011.03.018>
- Meyers, P. A., Bernasconi, S. M., & Forster, A. (2006). Origins and accumulation of organic matter in expanded Albion to Santonian black shale sequences on the Demerara Rise, South American margin. *Organic Geochemistry*, 37(12), 1816–1830. <https://doi.org/10.1016/j.orggeochem.2006.08.009>
- Naafs, B. D. A., Monteiro, F. M., Pearson, A., Higgins, M. B., Pancost, R. D., & Ridgwell, A. (2019). Fundamentally different global marine nitrogen cycling in response to severe ocean deoxygenation. *Proceedings of the National Academy of Sciences*, 116(50), 24979–24984. <https://doi.org/10.1073/pnas.1905553116>
- Ostrander, C. M., Owens, J. D., & Nielsen, S. G. (2017). Constraining the rate of oceanic deoxygenation leading up to a Cretaceous Oceanic Anoxic Event (OAE-2: ~94 Ma). *Science Advances*, 3(8), e1701020. <https://doi.org/10.1126/sciadv.1701020>
- Percival, L. M. E., Bond, D. P. G., Rakociński, M., Marynowski, L., Hood, A. v. S., Adatte, T., et al. (2020). Phosphorus-cycle disturbances during the Late Devonian anoxic events. *Global and Planetary Change*, 184, 103070. <https://doi.org/10.1016/j.gloplacha.2019.103070>
- Percival, L. M. E., Selby, D., Bond, D. P. G., Rakociński, M., Racki, G., Marynowski, L., et al. (2019). Pulses of enhanced continental weathering associated with multiple Late Devonian climate perturbations: Evidence from osmium-isotope compositions. *Palaeogeography, Palaeoclimatology, Palaeoecology*, 524, 240–249. <https://doi.org/10.1016/j.palaeo.2019.03.036>
- Pujol, F., Berner, Z., & Stüben, D. (2006). Palaeoenvironmental changes at the Frasnian/Famennian boundary in key European sections: Chemostratigraphic constraints. *Palaeogeography, Palaeoclimatology, Palaeoecology*, 240(1–2), 120–145. <https://doi.org/10.1016/j.palaeo.2006.03.055>
- Qie, W., Algeo, T. J., Luo, G., & Herrmann, A. (2019). Global events of the Late Paleozoic (Early Devonian to Middle Permian): A review. *Palaeogeography, Palaeoclimatology, Palaeoecology*, 531, 109259. <https://doi.org/10.1016/j.palaeo.2019.109259>
- Racki, G. (2020). A volcanic scenario for the Frasnian–Famennian major biotic crisis and other Late Devonian global changes: More answers than questions? *Global and Planetary Change*, 189, 103174. <https://doi.org/10.1016/j.gloplacha.2020.103174>
- Racki, G., Racka, M., Matyja, H., & Devleeschouwer, X. (2002). The Frasnian/Famennian boundary interval in the South Polish–Moravian shelf basins: Integrated event-stratigraphical approach. *Palaeogeography, Palaeoclimatology, Palaeoecology*, 181(1–3), 251–297. [https://doi.org/10.1016/S0031-0182\(01\)00481-3](https://doi.org/10.1016/S0031-0182(01)00481-3)
- Robinson, S. A., Heimhofer, U., Hesselbo, S. P., & Petrizzo, M. R. (2017). Mesozoic climates and oceans—A tribute to Hugh Jenkyns and Helmut Weissert. *Sedimentology*, 64, 1–15. <https://doi.org/10.1111/sed.12349>
- Ruvalcaba Baroni, I., van Helmond, N. A. G. M., Tsandev, I., Middelburg, J. J., & Slomp, C. P. (2015). The nitrogen isotope composition of sediments from the proto-North Atlantic during Oceanic Anoxic Event 2. *Paleoceanography*, 30(7), 923–937. <https://doi.org/10.1002/2014PA002744>
- Sageman, B. B., Murphy, A. E., Werne, J. P., Ver Straeten, C. A., Hollander, D. J., & Lyons, T. W. (2003). A tale of shales: The relative roles of production, decomposition, and dilution in the accumulation of organic-rich strata, Middle–Upper Devonian, Appalachian basin. *Chemical Geology*, 195(1–4), 229–273. [https://doi.org/10.1016/S0009-2541\(02\)00397-2](https://doi.org/10.1016/S0009-2541(02)00397-2)
- Sandberg, C. A., Morrow, J. R., & Ziegler, W. (2002). *Late Devonian sea-level changes, catastrophic events, and mass extinctions* (Vol. 356, p. 473–487). Geological Society of America Special Papers. <https://doi.org/10.1130/0-8137-2356-6.473>
- Sandberg, C. A., Ziegler, W., Dreesen, R., & Butler, J. L. (1988). Late Frasnian extinction: Conodont event stratigraphy, global changes, and possible causes. *Courier Forschungsinstitut Senckenberg*, 102, 263–307.
- Schubert, C. J., & Calvert, S. E. (2001). Nitrogen and carbon isotopic composition of marine and terrestrial organic matter in Arctic Ocean sediments: Implications for nutrient utilization and organic matter composition. *Deep Sea Research Part I: Oceanographic Research Papers*, 48(3), 789–810. [https://doi.org/10.1016/S0967-0637\(00\)00069-8](https://doi.org/10.1016/S0967-0637(00)00069-8)
- Sigman, D. M., & Fripiat, F. (2019). Nitrogen isotopes in the ocean. In J. Cochran, H. Bokuniewicz, & P. Yager, (Eds.), *Encyclopedia of ocean sciences* (3rd ed., pp. 263–278). Elsevier.
- Song, H., Song, H., Algeo, T. J., Tong, J., Romaniello, S. J., Zhu, Y., et al. (2017). Uranium and carbon isotopes document global-ocean redox-productivity relationships linked to cooling during the Frasnian-Famennian mass extinction. *Geology*, 45(10), 887–890. <https://doi.org/10.1130/G39393.1>

- Spalletta, C., Perri, M. C., Over, D. J., & Corradini, C. (2017). Famennian (Upper Devonian) conodont zonation: Revised global standard. *Bulletin of Geosciences*, 92, 31–57. <https://doi.org/10.3140/bull.geosci.1623>
- Summons, R. E., & Jahnke, L. L. (1990). Identification of the methylhopanes in sediments and petroleum. *Geochimica et Cosmochimica Acta*, 54(1), 247–251. [https://doi.org/10.1016/0016-7037\(90\)90212-4](https://doi.org/10.1016/0016-7037(90)90212-4)
- Summons, R. E., Jahnke, L. L., Hope, J. M., & Logan, G. A. (1999). 2-Methylhopanoids as biomarkers for cyanobacterial oxygenic photosynthesis. *Nature*, 400(6744), 554–557. <https://doi.org/10.1038/23005>
- Summons, R. E., & Powell, T. G. (1987). Identification of aryl isoprenoids in source rocks and crude oils: Biological markers for the green sulphur bacteria. *Geochimica et Cosmochimica Acta*, 51(3), 557–566. [https://doi.org/10.1016/0016-7037\(87\)90069-X](https://doi.org/10.1016/0016-7037(87)90069-X)
- Sun, Y. D., Zulla, M. J., Joachimski, M. M., Bond, D. P. G., Wignall, P. B., Zhang, Z. T., & Zhang, M. H. (2019). Ammonium Ocean following the end-Permian mass extinction. *Earth and Planetary Science Letters*, 518, 211–222. <https://doi.org/10.1016/j.epsl.2019.04.036>
- Szulczewski, M. (1996). Devonian succession in the Kowala quarry and railroad cut. In *Sixth European conodont symposium (ECOS VI)* (p. 27–30).
- Taylor, S. R., & McLennan, S. M. (1995). The geochemical evolution of the continental crust. *Reviews of Geophysics*, 33(2), 241–265. <https://doi.org/10.1029/95RG00262>
- Thunell, R. C., Sigman, D. M., Muller-Karger, F., Astor, Y., & Varela, R. (2004). Nitrogen isotope dynamics of the Cariaco Basin, Venezuela. *Global Biogeochemical Cycles*, 18(3). <https://doi.org/10.1029/2003GB002185>
- Tuite, M. L., Williford, K. H., & Macko, S. A. (2019). From greenhouse to icehouse: Nitrogen biogeochemistry of an epeiric sea in the context of the oxygenation of the Late Devonian atmosphere/ocean system. *Palaeogeography, Palaeoclimatology, Palaeoecology*, 531, 109204. <https://doi.org/10.1016/j.palaeo.2019.05.026>
- Uveges, B. T., Junium, C. K., Boyer, D. L., Cohen, P. A., & Day, J. E. (2019). Biogeochemical controls on black shale deposition during the Frasnian-Famennian biotic crisis in the Illinois and Appalachian Basins, USA, inferred from stable isotopes of nitrogen and carbon. *Palaeogeography, Palaeoclimatology, Palaeoecology*, 531, 108787. <https://doi.org/10.1016/j.palaeo.2018.05.031>
- Voss, M., Emeis, K. C., Hille, S., Neumann, T., & Dippner, J. W. (2005). Nitrogen cycle of the Baltic Sea from an isotopic perspective. *Global Biogeochemical Cycles*, 19(3). <https://doi.org/10.1029/2004GB002338>
- Wada, E., Minagawa, M., Mizutani, H., Tsuji, T., Imaizumi, R., & Karasawa, K. (1987). Biogeochemical studies on the transport of organic matter along the Otsuchi River watershed, Japan. *Estuarine, Coastal and Shelf Science*, 25(3), 321–336. [https://doi.org/10.1016/0272-7714\(87\)90075-8](https://doi.org/10.1016/0272-7714(87)90075-8)
- Welander, P. V., Coleman, M. L., Sessions, A. L., Summons, R. E., & Newman, D. K. (2010). Identification of a methylase required for 2-methylhopanoid production and implications for the interpretation of sedimentary hopanes. *Proceedings of the National Academy of Sciences of the United States of America*, 107(19), 8537–8542. <https://doi.org/10.1073/pnas.0912949107>
- Whalen, M. T., Śliwiński, M. G., Payne, J. H., Day, J. E., Chen, D., & Da Silva, A. C. (2015). Chemostratigraphy and magnetic susceptibility of the Late Devonian Frasnian–Famennian transition in western Canada and southern China: Implications for carbon and nutrient cycling and mass extinction. In A. C. Da Silva, M. T. Whalen, J. Hladil, L. Chadimova, D. Chen, S. Spassov, et al., (Eds.), *Magnetic susceptibility application: A window onto ancient environments and climatic variations* (Vol. 414, p. 37–72). Geological Society, London, Special Publications. <https://doi.org/10.1144/SP414.8>
- White, D. A., Elrick, M., Romaniello, S., & Zhang, F. (2018). Global seawater redox trends during the Late Devonian mass extinction detected using U isotopes of marine limestones. *Earth and Planetary Science Letters*, 503, 68–77. <https://doi.org/10.1016/j.epsl.2018.09.020>
- Witzke, B. J., & Bunker, B. J. (2002). Bedrock geology in the Burlington area, southeast Iowa. In *Iowa geological Survey guidebook*, 23, p. 23–48.
- Zhang, X., Gao, Y., Chen, X., Hu, D., Li, M., Wang, C., & Shen, Y. (2019). Nitrogen isotopic composition of sediments from the eastern Tethys during Oceanic Anoxic Event 2. *Palaeogeography, Palaeoclimatology, Palaeoecology*, 515, 123–133. <https://doi.org/10.1016/j.palaeo.2018.03.013>
- Zhang, X., Sigman, D. M., Morel, F. M. M., & Kraepiel, A. M. L. (2014). Nitrogen isotope fractionation by alternative nitrogenases and past ocean anoxia. *Proceedings of the National Academy of Sciences of the United States of America*, 111(13), 4782–4787. <https://doi.org/10.1073/pnas.1402976111>